



UNIVERSITY OF NAIROBI

SCHOOL OF PHYSICAL SCIENCES

**SURFACE MODIFIED ELECTRODES USED AS NANO-ELECTROANALYTICAL
TOOL-IN THE ELECTROCHEMICAL-PROFILING OF HYDROCORTISONE
(MEDICATED CREAM), TOP LEMON AND EXTRA CLAIR (BEAUTY CREAMS)**

DORCAS GATHONI NGIGI

I56/87609/2016

MSc. CHEMISTRY

DEPARTMENT OF CHEMISTRY

UNIVERSITY OF NAIROBI

**A thesis submitted in partial fulfillment of the requirement for the award of Master of
Science Degree in Chemistry of the University of Nairobi**

October 2019

DECLARATION

I declare that this thesis has not been submitted for academic award in any other University. Where information has been sourced from other people's work, authors have been acknowledged, proper citations have been used and the work has been referenced in accordance with the University of Nairobi's requirements

Sign..... Date.....

DORCAS GATHONI NGIGI

Department of Chemistry

School of physical sciences

University of Nairobi

This thesis has been submitted with our approval as research supervisors

PROF. DUKE ORATA

DR. VINCENT OCHIENG

PROFESSOR OF PHYSICAL CHEMISTRY

LECTURER

DEPT. OF CHEMISTRY

DEPT. OF BIOCHEMISTRY

Sign: _____

Sign: _____

Date: _____

Date: _____

UNIVERSITY OF NAIROBI

DEDICATION

I dedicate this thesis to all my family members who have given me their unwavering support during the period of study. This appreciation goes especially to my parents Ngigi and Wahu, my husband Omondi and our children Grace, Karanja and Esther.

I thank the Almighty God who through His grace and mercy, I have been able to complete the program.

ACKNOWLEDGEMENTS

I must first start by thanking the Almighty God who gives us the ability to accomplish tasks in life through His grace.

I thank the Department of Chemistry University of Nairobi which was the host department during the program, and also thank all staff members in the department of chemistry both academic and technical staff for their support during the program.

I especially thank my supervisors Prof. Duke Orata and Dr. Vincent Ochieng for the support and guidance during the project.

I also thank the College of Biological and Physical Sciences, School of Physical Sciences, Board of Examiners and the Graduate School who were involved in the processing and examination of this thesis.

Finally and more importantly, I thank my parents Wahu and Ngige, my husband Omondi and children Grace, Harrison and Esther for their unwavering support for all my endeavors.

TABLE OF CONTENTS

DECLARATION -----	i
DEDICATION-----	ii
ACKNOWLEDGEMENTS-----	iii
TABLE OF ABBREVIATIONS-----	ix
LIST OF FIGURES-----	x
LIST OF SCHEMES-----	xvii
LIST OF TABLES-----	xvi
LIST OF APPENDIX -----	xviii
ABSTRACT-----	xix
CHAPTER ONE-----	1
1.1 Background to the study-----	1
1.1.1 Medicated creams and ointment-----	1
1.1.2 Composition, Pharmacology, pharmacokinetics and drug interactions-----	2
1.1.3 Complexion/skin toning creams -----	2
1.2 Statement of the problem-----	3
1.3 Objectives of the study-----	3
1.4 Justification of the study-----	4
1.5 Significance of the study-----	4

CHAPTER TWO	-----5
LITERATURE REVIEW	-----5
CHAPTER THREE	----- 18
RESEARCH MATERIALS AND METHODOLOGY	-----18
3.0 Instrumentation for cyclic voltammetry	-----18
3.3 Electrode assembly	-----23
3.3.1 Reference electrode	-----23
3.4.1 Sample preparation	-----25
3.4.2 Chemical reagents	-----25
3.4.3 Glassware	-----25
CHAPTER FOUR	-----28
RESULTS AND DISCUSSIONS	-----28
4.1 Electrochemical studies on top lemon- beauty cream	-----28
4.1.1 Modification of Carbon Graphite Working Electrode with Top Lemon Cream	-----28
4.1.2 Top lemon modified carbon graphite electrode in Sodium Chloride supporting electrolyte	-----31
4.1.3 Top Lemon on Polyaniline modified carbon graphite electrode	-----32
4.1.4 Top lemon on Polyaniline Modified Electrode	----- 34
4.1.5 Effect of p-aminophenol on Top-lemon redox process on different host matrices	----- 40

4.1.6 Top lemon redox activity on a Bentonite	
Modified Electrode -----	42
4.1.7. Top lemon-bentonite composite modified electrode-----	43
4.2.1 Electro-analysis of the Redox Properties of	
4.2 Extra Clair Cream-----	45
i.Redox Activity of Extra Clair Cream on Bare Carbon	
graphite Electrode. -----	45
ii. Redox properties of Extra Clair cream on polyaniline	
modified electrode. -----	45
i) Electro-catalytic role of p-aminophenol in the Extra Clair	
redox process. -----	53
iv) Redox activity of Extra Clair cream on bare carbon graphite working	
electrode in the Presence of p-aminophenol-----	56
v) Redox activity of Extra Clair on Bentonite modified electrode-----	62
vi) Extra Clair cream –Bentonite composite on carbon	
graphite working electrode. -----	63
vii) Redox activity of Extra Clair cream on Polyaniline –	
Bentonite modified electrode-----	66
vii) Effect of p-aminophenol on the redox properties of Extra Clair	
cream-Bentonite composite modified electrode-----	68

4.3 Electrochemical analysis of hydrocortisone-medicated cream-----	73
i) Redox activity of Hydrocortisone on bare carbon graphite working electrode-----	73
ii) Hydrocortisone redox process in sodium chloride supporting electrolyte solution-----	74
iii) Redox behavior of Hydrocortisone on Polyaniline modified carbon graphite electrode. -----	76
iv) Electrochemical properties of Hydrocortisone on Bentonite modified electrode-----	80
v) Hydrocortisone-Bentonite composite as electrode modification material.-----	82
vii) Redox activity of Hydrocortisone modified carbon graphite electrode in the presence of p-aminophenol-----	83
4.4 FTIR spectrophotometric analysis -----	84
CHAPTER FIVE-----	88
5.1 Conclusion -----	88
5.2 Recommendations-----	88
REFERENCES-----	89

TABLE OF ABBREVIATIONS

CT-Catechol

CV-Cyclic Voltammogram

FTIR- Fourier Transform Infra-Red Spectra

HQ- Hydroquinone

HPLC- High Performance Liquid Chromatography

i –Current

e/E –Potential

ma-milliamperes

PANI- Polyaniline

PAR- Princeton Applied Research

SCE-Saturated Calomel Electrode

SHE- Standard Hydrogen Electrode

SME-Surface Modified Electrodes

Redox- Reduction/Oxidation

XRF-X-ray Fluorescence Spectroscopy

KEBS-Kenya Bureau of Standards

w/w- weight/weight

w/v-weight /volume

LIST OF FIGURES

Fig. 2: Structure of Carbon Surface

Figure 3.0: Schematic diagrams for operational amplifiers

Figure 3.1: Voltage amplifier

Figure 3.2: A current follower

Figure 3.3: An adder potentiostat with a positive feedback compensation

Figure 3.4: saturated calomel electrode (SCE)

Figure 3.5: A scheme of a XRF spectrometer

Figure 4.1: Cyclic voltammogram for Top-lemon modified electrode in 1.0 M sulphuric acid at a scan rate of 20mv/sec

Figure 4.2: Effect of solution pH on the Top-lemon redox process

Figure 4.3: The cyclic voltammetric response of Top-lemon in 1M NaCl at a scan rate of 10mV/sec

Figure 4.4: Cyclic voltammogram for Top-lemon on polyaniline modified electrode in 1M NaCl. Scan rates- 10mV/s, 20mV/s, 50mV/s and 100mV/s

Figure 4.5: Electrodeposition of polyaniline on carbon graphite electrode. Potential cycled from -0.3V to 0.85V, scan rate 20mV/s

Figure 4.6: CV response for Top lemon on polyaniline modified electrode in 1M sulphuric acid and 0.1M aniline. Scan rate 20mV/s

Figure 4.7: Effect of variation of positive potential limit of Top-lemon redox process.

Figure 4.8: CV response for Top-lemon on polyaniline modified electrode in electrolyte solution containing 2M HCl

Figure 4.9: Top lemon modified electrode in solution containing 0.01M p-aminophenol and 1M HCl. Potential cycled from -0.30V to 0.90V. Scan rate of 20mV/sec

Figure 4.10: CV response for p-aminophenol-Top-lemon modified electrode in 1M H₂SO₄. Potential range: -0.30V to 0.90V. Scan rate 20mV/s

Figure 4.11: CV response for Top-lemon on bentonite modified electrode. Potential range: -0.20V to 0.85V. Scan rate 20mV/s

Figure 4.12: CV response for Top lemon- bentonite composite electrode in 0.1M, 0.5M and 1.0M H₂SO₄. Potential range: -0.20V to 0.85V, scan rate 20mV/s

Figure 4.13: CV response for bentonite-polyaniline-Top lemon electrode in 1M H₂SO₄. Potential range:-0.3V (constant) to 0.70V, 0.75V, 0.80V, 0.85V and 0.90V. Scan rate 20mV/s.

Figure 4.14: CV response for Extra Clair modified electrode in 0.1M, 0.5M and 1.0M H₂SO₄. Potential range: -0.30V to 0.90V. Scan rate 20mV/s

Figure 4.15: Variation of scan rate studies for Extra Clair. Potential range:-0.30 V to 0.90V, Scan rates: 5mV/s, 10mV/s, 20mV/s, 50mV/s, 100mV/s.

Figure 4.16: CV response for Extra Clair- PANI in 1.0M NaCl. Potential range: -0.30 V to 0.70V, 0.80 V, 0.85V and 0.90V. Scan rate 20mV/s

Figure 4.17: CV response for Extra Clair- PANI in 0.1M NaCl. Potential range: -0.30 V to 0.70V, 0.80 V, 0.85V and 0.90V. Scan rates: 5mV/s, 10mV/s, 20mV/s, 50mV/s, 100mV/s.

Figure 4.18: Differences in the redox profile of Extra Clair-PANI in 0.1 M and 1.0M NaCl supporting electrolyte solution.

Figure 4.19: Effect of electrolyte solution (H_2SO_4) concentration on Extra Clair-PANI redox process.

Figure 4.20: Extra-Clair- PANI redox process in 1.0M HCl and 0.01M p-aminophenol. Scan rate 20mV/s, potential range: -0.30V to 0.90V

Figure 4.21: The effect of solution pH on the Extra Clair –PANI electrode

Figure 4.22: Redox activity of Extra Clair modified carbon graphite electrode in 1.0M HCl and 0.01M p-aminophenol

Figure 4.23: Figure 4.22: Redox activity of Extra Clair modified carbon graphite electrode in 1.0M H_2SO_4 and 0.01M p-aminophenol

Figure 4.24: Effect of solution pH on the redox activity of Extra Clair modified carbon graphite electrode in 0.1M and 0.5M sulphuric acid.

Figure 4.25: Redox activity of Extra Clair-Bentonite modified electrode in 1.0M sulphuric acid. Potential range -0.30V to 0.90V, scan rate 20mV/s

Figure 4.26: CV response of Extra Clair-Bentonite composite modified electrode in 0.1M, 0.5M and 1.0M sulphuric acid solutions. Potential range: -0.30V to 0.90V. Scan rate 20mV/s

Figure 4.27: Effect of anion type on the Extra Clair-bentonite composite redox process.

Figure 4.28: CV response of Bentonite/PANI/Extra Clair modified electrode in 1.0M sulphuric acid. Potential range: -0.30V to 0.90V. Scan rate 20mV/s

Figure 4.29: Effect of p-aminophenol on the Extra Clair-Bentonite composite redox process

Figure 4.30: CV response of Extra Clair-bentonite composite in 1.0M HCl. Potential range :0.30V to 0.90V. Scan rate 20mV/s

Figure 4.31: CV response of Extra Clair-bentonite composite in 10% acetonitrile: 90% water and 0.01M Tetrabutyl ammonium perchlorate (TBAP). Potential range: -0.30V to 0.90V. Scan rate 20mV/s

Figure 4.32: CV response of Hydrocortisone modified electrode in 0.1M, 0.5M and 1.0M H₂SO₄ solutions. Potential range: -0.30V to 0.90V. Scan rate 20mV/s

Figure 4.33: CV response of Hydrocortisone modified electrode in 0.1M, 0.5M and 1.0M NaCl solutions. Potential range: -0.30V to 0.90V. Scan rate 20mV/s

Figure 4.34: CV response of Hydrocortisone-PANI modified electrode in 0.1M, 0.5M and 1.0M H₂SO₄ solutions. Potential range: -0.30V to 0.90V. Scan rate 20mV/s

Figure 4.35 Effect of variation of positive potential limit on the Hydrocortisone-PANI modified electrode.

Figure 4.36: CV response of Hydrocortisone –PANI modified electrode in 0.1M, 0.5M and 1.0M NaCl solutions. Potential range: -0.30V to 0.90V. Scan rate 20mV/s

Figure 4.37: CV response of Hydrocortisone –Bentonite modified electrode in 1.0M sulphuric acid solution. Potential range: -0.30V to 0.90V. Scan rate 20mV/s

Figure 4.37: CV response of Hydrocortisone –Bentonite modified electrode in 1.0M sulphuric acid solution. Potential range: -0.30V to 0.90V. Scan rate 20mV/s

Figure 4.38: CV response of Hydrocortisone –PANI-Bentonite modified electrode in 1.0M sulphuric acid solution. Potential range: -0.30V to 0.90V. Scan rate 20mV/s

Figure 4.39: CV response of Hydrocortisone–Bentonite modified electrode in 1.0M NaCl solution. Potential range: -0.30V to 0.90V. Scan rate 20mV/s

Figure 4.40: CV response of Hydrocortisone–Bentonite modified electrode in 1.0M NaCl solution. Potential range: - 0.30V to 0.90V. Scan rate 20mV/s

Figure 4.41: CV response of Hydrocortisone modified electrode in solution containing 1.0M sulphuric acid and 0.01M p-aminophenol. Potential range: -0.30V to 0.90V. Scan rate 20mV/s

Figure 4.42: FTIR spectral data for Top lemon

Figure 4.43: FTIR spectral data for Extra Clair

Figure 4.44: FTIR spectral data for Hydrocortisone

LIST OF TABLES

Table 2.1: Composition of Amboseli and Wyoming bentonite obtained from mineralogical and X-ray tests.

Table 3.1: Elemental composition of raw bentonite

Table 4.1: Effect of pH on the redox potentials

LIST OF SCHEMES

Scheme 1: Propagation of Polaron through a conjugated polymer chain by shifting of double bonds.

Scheme 2: Formation of polaron and bipolaron in polypyrrole

Scheme 3: Formation of two charged solitons from dissociation of bipolaron from transpolyacetylene.

Scheme 4: Polyaniline oxidation states

Scheme 5: Attachment to a carbon electrode after activation of thermally oxidized glassy carbon electrode.

(xvii)

LIST OF APPENDICES

Calculation of the electro-gravimetric weight of hydroquinone in Top-lemon

(xviii)

ABSTRACT

In this thesis, surface modified electrodes were used to study hydrocortisone cream (medicated cream), Top lemon and Extra Clair (beauty creams). The results presented show that in the 1.0 M sulphuric acid supporting electrolyte the oxidation/reduction peak potentials versus saturated calomel electrode (SCE) for the Top Lemon occurred at 0.61V/0.21V. The Extra Clair had a broad oxidation peak and a reduction peak at 0.44V while Hydrocortisone had a reduction peak at approximately 0.61 V.

The cyclic voltammetric responses obtained for Top lemon and Extra Clair beauty creams confirm the presence of quinonic peaks.

The results from charge calculations obtained from the cyclic voltammograms gave the electrogravimetric value of the Quinone as $6.1 \times 10^{-9} \text{ g/cm}^2$; this gives the percentage Quinone in the Top-lemon cream as 0.0001%. This falls within the acceptable hydroquinone limits in beauty creams. The total mass of cream in the Top-lemon in the tube was 15g net weight. The electro-gravimetric amount of hydroquinone in the tube is $3.75 \times 10^{-5} \text{ g}$. This result is significant in that it shows that surface modified electrodes can be used in determination of quantities of hydroquinone in beauty creams.

Top lemon is also shown to inhibit the polyaniline electro-degradation process.

The carbon graphite working electrode was further modified with electronically conducting polymer – polyaniline. This polymer can be switched from insulating to conducting state by varying the potential. The redox properties of Hydrocortisone, Top-lemon and Extra Clair were significantly altered.

The results also indicate that modification of the carbon-graphite working electrode with bentonite, a clay montmorillonite with a structured lattice having octahedral and tetrahedral sites affect significantly the redox processes associated with Hydrocortisone, Top lemon and Extra Clair. The Extra Clair oxidation/reduction peaks are well defined and occur at 0.84V/0.48V. The Top lemon had oxidation/reduction peaks at 0.58V/0.28V. The Hydrocortisone had broad misshapened peaks. The effect of the bentonite host matrix is attributed to pre-concentration, structural and entropic effects which represent the ‘Nano’ -electrochemical behavior of these host-matrices.

It has also been shown that the nature of cations and anions affect the redox properties of the creams referred to above. This has been attributed to protonation-deprotonation equilibria in the case of polyaniline host matrix. In bentonite the cationic effect is attributed to isomorphous substitution of the cations into the octahedral-layer of the bentonite host matrix. The anionic effect is associated with ionic radii and charge density

(xix)

p-Aminophenol has also been shown to affect the redox properties of the Hydrocortisone, Top-lemon and Extra Clair.

FTIR spectrophotometric analysis confirms the presence of hydroxyl, ketonic, aliphatics and aromatic functional groups in Hydrocortisone, Top lemon and Extra Clair.

CHAPTER ONE

INTRODUCTION

1.1 Background to the study

In general phenolic compounds such as catechol and hydroquinone are toxic and are harmful to animals and human beings even at very low concentrations. Unfortunately, these organic materials find a lot of use in the pharmaceutical industries, in beauty products and in tanning industries. In addition catechol and hydroquinone are detected in tobacco smoke. Thus, hydroquinone and catechol are not only a threat to human health but are also environmental pollutants. It has therefore become necessary to develop analytical methods which can accurately determine the quantities of hydroquinone and catechol (Wikipedia, Internet)

Among the techniques which have been used in the analysis of hydroquinone and catechol include spectrophotometry and high performance liquid chromatography. Derivatised electrodes are also being explored as alternative analytical tool (Bhaksi and Rattan, 1990; Bard and Villemure, 1990; Carter and Bard, 1986).

These derivatised electrodes also christened as surface modified electrodes (SME) have been used in the analysis of a broad range of chemical substances which have redox active centres (Bontidean et al.2003; Chow and Gooding, 2006; Daisuke and Susumu, 2007; Adriana et al. 2006; Orata et al.1987, 1992,1999, and 2014)

1.1.1 Medicated Creams and Ointments

Creams are for external use and are applied to the skin. They are mostly pharmaceutical products or cosmetic creams. In general creams are semi-solid emulsions characterized by the following two main types:

Oil-in-water (O/W) creams: These are used in cosmetics and are basically droplets of oil dispersed in a continuous phase. They are normally less greasy and can be washed off with water.

Water-in-oil (W/O) creams: These are normally droplets of water in a continuous oily phase. They are similarly less greasy and are easily washed off with. Creams are normally hydrophobic and moisturizing. They reduce water loss from the skin by providing an oily barrier on the skin.

1.1.2 Composition, pharmacology, pharmacokinetics and drug interaction:

Hydrocortisone Cream and Ointment: This cream is used for the control of various inflammatory skin disorders e.g., neuro dermatitis, eczema, atopic dermatitis and certain forms of psoriasis characterized by inflammation. This cream contains 10mg/g (1% w/w) hydrocortisone according to manufacturer pharmacological information and instructions enclosure contained in the cream package.

Pharmacology: Hydrocortisone anti-inflammatory action is through inhibition of specific functions of leukocytes. It achieves this by inhibiting the synthesis and release of prostaglandins, leukotrienes, platelet activating factor, interleukin-1 and tumor necrosis. In general hydrocortisone has antipruritic, anti-allergic and anti-inflammatory properties.

Pharmacokinetics: Hydrocortisone is absorbed through the skin, and can be applied occlusive dressings. The absorbed hydrocortisone is metabolized in the liver and most body tissues. The degraded forms such as tetrahydrocortisol and tetrahydrocortisone are excreted in urine mostly conjugated as glucuronides.

1.1.3 Complexion/skin toning creams:

Top Lemon Crème and Extra Clair Crèmes are popular complexion creams purchased from retail outlets without any prescription requirements. They are indicated to give a smooth extra Lightening complexion. The top crème has active antiseptic component which clears spots and blemishes. The Extra Clair Crème is indicated to have hydroquinone. These products are popular in the local market. Top-lemon especially has no composition data, and no detailed pharmacology and pharmacokinetics information. These beauty creams as at the time of carrying out this research analysis and writing the Thesis did not bare the diamond quality mark of the Kenya Bureau of Standards (KEBS).

Kenya Bureau of Standards is a government institution in the Republic of Kenya mandated to verify the quality of all local and imported products and approve their release into the market. The absence of the diamond quality mark therefore casts aspersions on the acceptability of these products in the Kenyan market.

1.2 Statement of the problem

The desire to look beautiful and elegant has led to an increase in the demand for beauty products worldwide. This has to an increased desire among a good number of women to have a lighter skin. This in turn has led to an increase in the demand for skin lightening beauty products. Unfortunately, most of these women especially in developing countries do not have financial ability to buy skin lightening products with no harmful ingredients. This has led to beauty cream manufacturers incorporating cheap and harmful substances such as hydroquinone in these cheap beauty products, in order to meet the high demand for these cheap skin lighteners. These harmful additives among others e. g steroids, mercury, oxidants have been added to beauty products by manufactures.

Major effects of these substances include carcinogenic reactions as well as causing mucous membrane and irritation. Steroids cause skin thinning, aggressiveness and mood swings among other effects, while mercury accumulation in the body organs leads to death as it is very toxic.

It is therefore imperative to carry out this study that seeks to establish how modified electrodes can be used in the qualitative and quantitative profiling of electroactive groups in beauty and medicated creams.

1.3 Objectives of the study

The main focus in this study will be to analyze the presence of the hydroquinone in two selected beauty products- Top lemon and Extra Clair by the use of surface modified electrodes technique.

The electrochemical properties of Hydrocortisone, Top-lemon and Extra Clair will be studied by deliberate modification of the carbon graphite working electrode, so that, the electrode displays the electrochemical features of the modifiers.

The carbon graphite working electrode surface will be modified with electronically conducting polymer-polyaniline and clay montmorillonite-bentonite. The effect of these host-matrices on the redox profile of Hydrocortisone, Top-lemon and Extra Clair will be studied.

1.3.1 Specific objectives

- i. To study the electrochemical response of Top-lemon, Extra Clair (Beauty creams) and Hydrocortisone (Medicated creams) Modified Electrode.

- ii. To obtain the optimum electrolytic conditions for optimum electrolytic response.
- iii. To study the effect of nature of supporting electrolyte, solution pH, scan rate, and rate limiting steps on the Hydrocortisone, Top-lemon and Extra Clair redox processes
- iv. Study removal of oxidative stress in the Hydrocortisone, Top-lemon and Extra-Clair redox systems through the electro catalytic action of p-amino phenol

1.4 Justification of the study

The process of detecting qualitatively and quantitatively hydroquinone in beauty creams poses a major challenge in laboratories. The use of surface modified electrodes as a **novel** alternative analytical tool is significant. This method is fast, specific and cost-effective.

1.5 Significance of the study

Detection of very low quantities of redox active analytes in Top-lemon, Extra Clair and Hydrocortisone using surface modified electrodes will be a new frontier in 'nano' electroanalysis. This new electro-analytical tool will effectively assess the integrity and quantity of redox active moieties in a broad range of restricted/and or rogue pharmaceutical products circulating in the Kenyan market.

CHAPTER TWO

LITERATURE REVIEW

2.1 SURFACE MODIFIED ELECTRODES

2.1.1 Introduction

Surface modified electrodes also referred to as derivatized electrodes have been the subject of intense research spanning all areas in applied electrochemistry ranging from rechargeable batteries, electrochromic display devices, electrochemical assessment of pharmaceutical products, biosensors etc.(Orata et al., 2014 and references therein).

Electrode surface modification refers to the process of immobilizing a chemical substance on the working electrode surface, so that the latter displays the electrochemical properties of the immobilized species.

This working electrode must therefore be interfaced to an electrochemical unit which gives the corresponding electrochemical signal resulting from redox activities taking place in the modified electrode. The electrochemical technique used commonly in the study of surface modified electrodes is cyclic voltammetry.

The cyclic voltammograms generated from cyclic voltammetry give the requisite information on the redox processes associated with the redox active analyte in the substance used in the electrode modification (Orata et al, 2014).

Successful application of surface modified electrodes requires that the immobilized species have redox active moieties, can be adsorbed physically or chemically on the electrode surface and to have low solubility in the supporting electrolyte media. The working electrode does not have to be exclusively

carbon graphite or glassy carbon, but can be a gold electrode as was the case in the Quartz Crystal Microbalance analysis of the conducting polymer-polyaniline, platinum or an optically transparent electrode (Bard et al, 1986; Buttry and Orata,1987;Lane and Hubbard, 1973)._The data obtained from surface modified electrodes are very specific and precise in the identification of the nature and type of the redox active moiety. The surface modified electrode can be studied under different electrochemical conditions such as different supporting electrolyte (acids and salts), solutions of different pH's, different types of solvents i.e., aqueous and non-aqueous (Orata et al, 1992, 2014; Adams R.W, 1969; Arnold and Murphy, 1965; Bard and Rudzinski, 1986; Carter and Bard, 1986; Elliot and Murray, 1976; Ghosh and Bard, 1983; Ege et al. 1984).

The data obtained from the interfaced electrochemical unit for example in the case of cyclic voltammetry will lead to the computation of oxidation and reduction charges, quantities which are used in the calculation of surface coverage and the electro-gravimetric weight of the redox species. In the case of Quartz Crystal Microbalance, the frequency changes on loading the electrode for example, during electrodeposition of the polymer, allows computation of the quantities electrodeposited ((Buttry and Orata ,1987).

Surface modified electrodes have also been used to study pharmaceutical products such as Amoxicillin, Pyrimethamine/2-sulfalido-3-methoxypyrazine and Lumefantrine/Artemeter, N

Acetyl P-Aminophenol, Quinine etc. (Orata D., Yusuf A., Nineza C.,(2014); Orata D., Yusuf A., Nineza C., Mukabi M., Njenga H.,Mbui D.,(2014).

2.1.2. Electrode Modification Methods

Chemisorption, covalent bonding and derivatization by film formation are the most popular methods used in immobilizing chemical substances on the working electrode surface. (Arnold and Murphy, 1965; Elliot and Murray 1976; Lane and Hubbard, 1973)

2.1.2.1 Chemisorption

The material to be modified is usually Pt electrode, metal oxide electrode and carbon graphite electrode.

Chemisorption unlike physi-sorption which are relatively weak reversible bonds, refers to strong irreversible adsorption of the electroactive substances on the electrode surface. These are strong valence forces similar to those found in the formation of chemical compounds. Examples include the adsorption of olefinic compounds on Pt, a process achieved by soaking the Pt in a dilute solution of the organic compound (Hubbard and Lane, 1973).

As already mentioned the electrode displayed the redox properties of the chemisorbed substance. Chemisorption on electrodes alters their properties (Arnold and Murphy, 1965).

When carbon electrode is used in the modification, it is noted that, the chemical and electrochemical nature of the immobilized species becomes significant (Anson and Oyama, 1980) and more chemically diverse than those on Pt. On the carbon electrode there is interaction of molecules having extended pi-electron systems with basal plane pyrolytic graphite.

2.1.2.2 Covalent Bonding

Chemically reactive substances were immobilized on optically transparent electrodes, a good example being SnO₂ electrode. This electrode has many Sn-OH sites which can react with reactive chlorosilanes, alkoxy silanes etc. This modification is achieved by exposing the optically transparent electrode to a solution of dichloromethylsilane under anhydrous conditions. The immobilization

results from the formation of SnOSi-bonds. This immobilization procedure is referred to as silanization (Lane and Hubbard, 1973)

2.1.3 Clay Modified Electrodes (CME)

2.1.3.1 Clay montmorillonite

Clay montmorillonites have been used extensively in electrode modification. Bentonite for example is known to have an orderly structure with tetrahedral and octahedral sheets. In the clay structure we also have the interlamellar layer and basal spacing. The octahedral layer is normally occupied by Al or Mg.

Examples include Smectite clays also referred to as 2:1 phyllosilicates because of the 2:1 relation between the tetrahedral and octahedral sheets within a layer.

In addition to this well-defined layered structure, clay has flexible adsorption properties and potential as catalyst and/or catalyst supports. Clays have high thermal and chemical stability, different composition and particle size. Clay films normally contain many defects such as holes and pores of varying size suggesting the presence of different adsorption sites (Bard and Villemure, 1990).

2.1.4. Bentonite

2.1.4.1 Mineralogy

Bentonite is a clay montmorillonite and has Na^+ or Ca^{2+} as the isomorphously substitutable ion. Bentonite has very high swelling capacities and colloidal properties. The general formula of Bentonite is represented as $\text{M}(\text{Al}, \text{Fe}, \text{Mg})_4(\text{Al}, \text{Si})_8\text{O}_{20}(\text{OH})_4n\text{H}_2\text{O}$

2.1.4.2 Bentonite Occurrences in Kenya

In Kenya Bentonite occurs at Amboseli, Nanyuki and Athi River. Bentonite from Amboseli contain mainly sepiolite, dolomite, calcite and illite (Williams, 1972) with montmorillonite found only in few samples. Chemical analysis of the Amboseli, Nanyuki, Athi River and Wyoming bentonite is shown in table 2.1.

Table 2.1: Composition of Amboseli, Nanyuki, Athi River and Wyoming bentonite obtained from mineralogical and X-ray tests.

Oxide	%composition			
	1	2	3	4
SiO ₂	45.70	42.02	41.32	57.98
CaO	9.70	5.62	6.25	1.92
MgO	5.52	10.12	10.57	3.24
Na ₂ O+K ₂ O	3.96	6.84	6.42	1.35

2.1.4.3 Clay modified electrodes

Clay modified electrodes have been the subject of intense research and result from modification of the working electrode surface with a thin layer of clay. The clay modified electrode has adsorption and/or catalytic properties which improve the selectivity or the sensitivity of the electrodes toward solution species (Ghosh and Bard, 1983)

Clay modified electrodes have been shown to improve the electrochemical signal of redox active species as compared to those witnessed at bare electrodes by pre concentration of the analyte in its matrix.

Example of enhanced peak currents were found in the cyclic voltammograms of clay adsorbed metal bipyridylcations (Bard and Villemure, 1990).

It is important to note that only a small fraction of the total species contained in the clay is electroactive (Carter and Bard, 1986; Ege, *et.al*, 1984). The species in the interlamellar spaces are thought not to be electroactive (Bard and Rudzinski, 1986). This ensures limited redox interference hence clay modified electrodes can be used as a host matrix on the working electrode in the study of other redox species.

Simple dry or spin coating from colloidal solution suspension is the most common method of applying clay to an electrode surface (Heinze and Merz, 1990).

2.1.5 Conducting Polymers Modified Electrodes

2.1.5.1 Band Theory

The band theory which involves the formation of Molecular orbitals from the overlap of atomic orbitals of atoms with similar orbitals of neighboring atoms, has been the foundational explanation for conduction in polymers. The many molecular orbitals form what looks like continuous energy bands. The band gap is the energy spacing between the highest occupied and lowest unoccupied bands called valence band and conduction band.

The partially occupied bands, conduction band and empty valence band or a zero band gap are responsible for the high conductivity of metals.

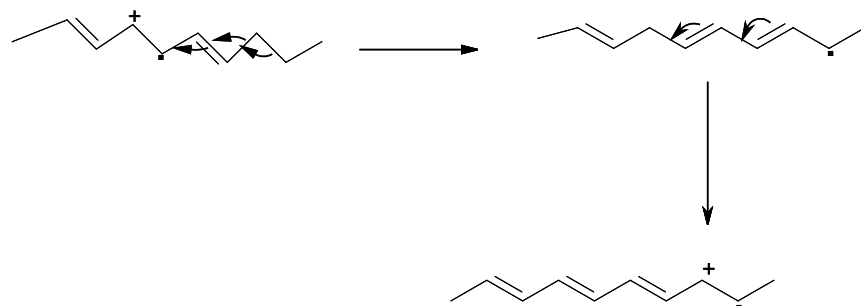
On the other hand electronically conducting polymers such as polyaniline, polythiophene, polypyrrole etc. conduct current without having a partially empty or partially filled band. It is therefore apparent that electrical conductivity in these organic conductors cannot be explained well by the simple band theory. In organic conducting polymers conduction or charge transport is thought to be as a result of movement of polarons and bipolarons. This concept explains very well the optical absorption changes seen in these polymers with doping.

2.1.5.2 Mechanism of Polarons

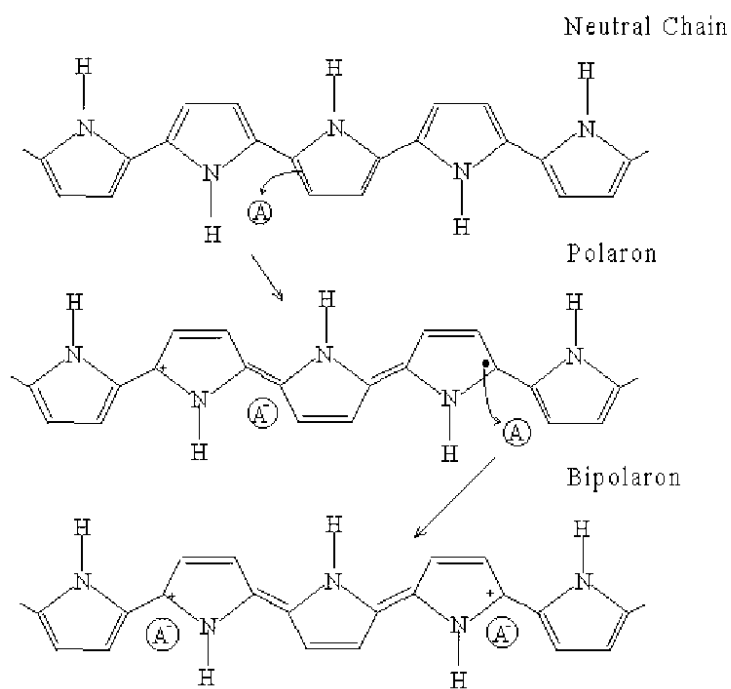
When an electron is removed from the top of the valence band of a conjugated polymer (e.g. polyacetylene, polypyrrole) a hole or radical cation is created that does not delocalize completely. Partial delocalization which extends over several monomeric units causes them to deform structurally. These radical cations can be considered to be destabilized bonding orbitals, with their energy slightly higher i.e. is in the band gap. When a radical cation is partially delocalized over some polymer segment it is called a polaron. It polarizes the medium around it, The removal of another electron from the already oxidized polymer containing the polaron leads to the creation of another independent polaron. The removal of unpaired electron from the first polaron level lead to formation of a special dication called bipolaron.

The dissociation of bipolaron can lead to the formation of two solitons as seen in the case of transpolyacetylene.

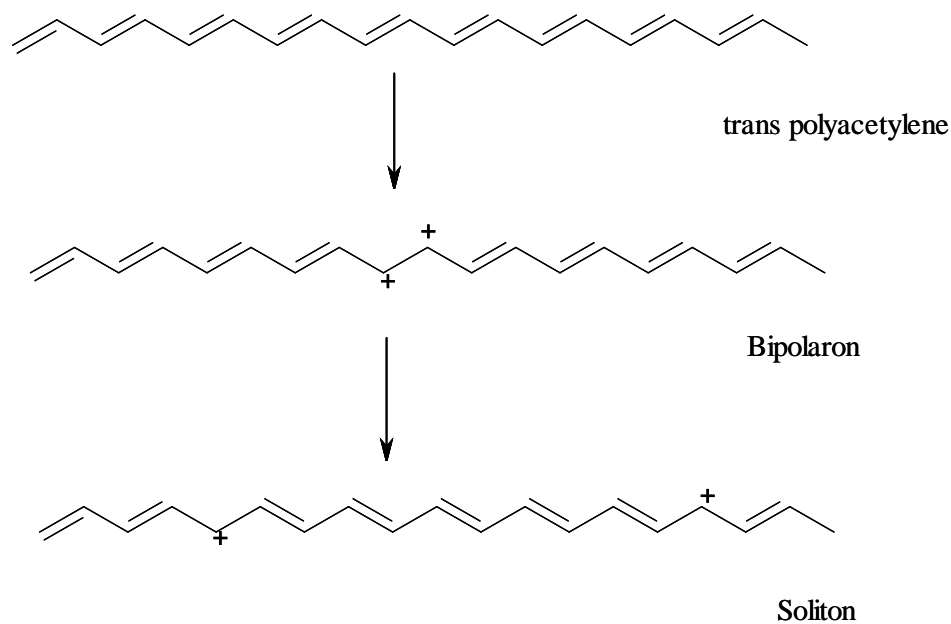
Polarons and bipolarons move along the polymer chain by the rearrangement of double and single bonds in the conjugated system that occurs in an electric field.



Scheme 1: Movement/or propagation of a polaron through a conjugated polymer chain by shifting of double bonds



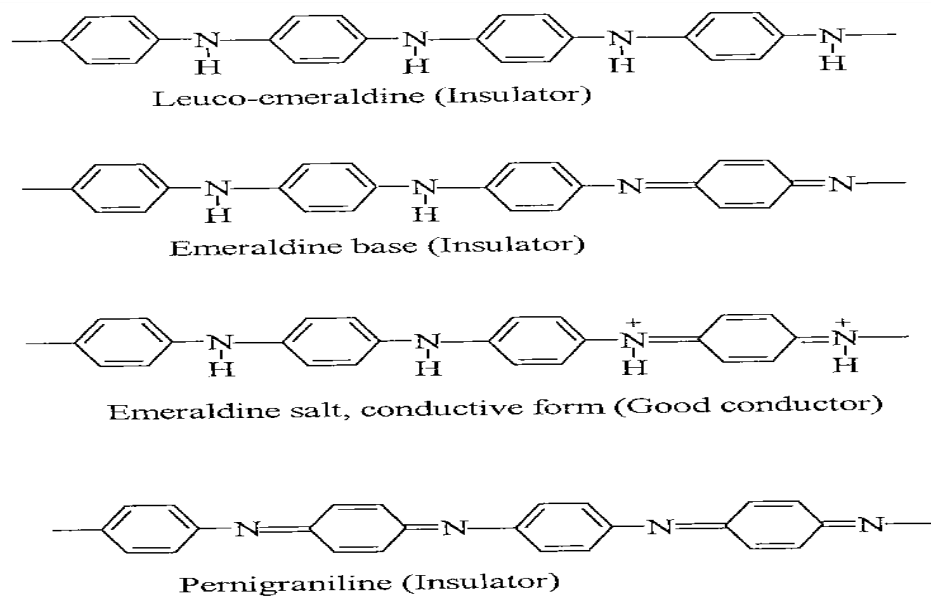
Scheme 2: Formation of polaron and bipolaron in polypyrrole



Scheme 3: Formation of two charged solitons from dissociation of bipolaron from transpolyacetylene.

2.1.5.3 Polyaniline

Polyaniline is generated from electrodeposition/ polymerization of aniline monomers. It can consist many aniline repeating units. Its electrical conductivities varies from 10^{-11} to more than 10 S/cm.



Scheme 4: Polyaniline oxidation states

Different compositions of polyaniline have different colors and electrical properties. The emeraldine salt is electrically conducting. By dipping the emeraldine films in acid, the imine nitrogen in the backbone of the polymer become protonated. Treated with aqueous alkali, the conductive emeraldine salt becomes insulating. The conductivity of the polymer depends on the pH of the solution it is treated with. Extensive research has been conducted on polyaniline and other electronically conducting polymers such as polypyrrole and polythiophene (Orata et al., 2014) and especially their role as host matrix for studying the redox processes of other chemical substances. **2.1.5.4 Applications**

Some of the applications of conducting polymers include use in rechargeable batteries, electrochromic display systems, drug release systems, biochemical biosensors, light emitting diodes, artificial nerves and electromagnetic shielding (Bakhshi and Rattan, 1997; Riul, *et.al*,2003).

2.1.6 Modification of the carbon electrodes

2.1.6.1 Chemical nature of carbon surface

Carbon graphite is the most widely used electrode. This is as a result of the following properties:

- Good electrical conductivity
- Corrosion resistance
- High purity
- Thermal conductivity.

Chemically, carbon graphite consists of fused aromatic rings, stacked coplanarly with a continuous basal plane surface which is non- ionic and of low polarity, hydrophobic, and rich in pi- electron density (Elliot and Murray, 1976; Firth B.E et al, 1976).

The strong chemisoptive interaction of carbon graphite especially with unsaturated compounds including aromatic ones is the result of the high pi-electron density (Anson and Brown, 1977).

Pyrolytic graphite is a highly imperfect approximation to single crystal graphite with a basal edge plane surface. Glassy carbon consist of graphite strips so that any given exposed surface exhibits a mixture of basal and edge plane characteristics. Polishing and pretreatment of the carbon electrode surface changes the characteristics of its surface (Lennox and Murray, 1977).

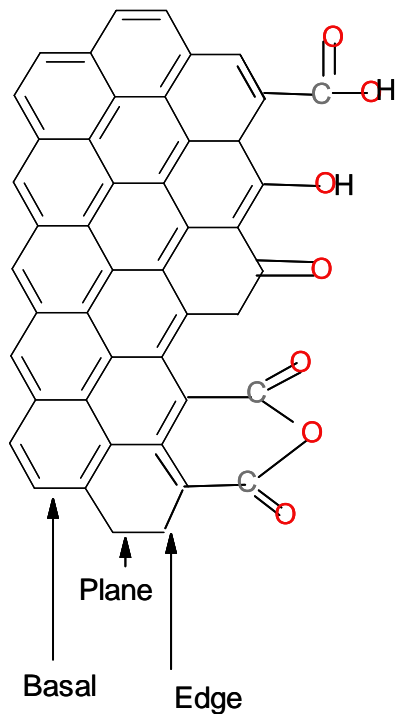


Fig. 2: Structure of Carbon Surface

2.1.7. Applications of Surface Modified Electrodes

2.1.7.1 Preconcentration Methods

Modified electrode surface can act as preconcentrating surfaces in which the analyte species is collected and concentrated on the electrode by chemical reactions with the groups attached to the electrode. Then the analyte is measured by the electrochemical response to a potential step or sweep (Lane and Hubbard, 1973)

2.1.7.2 Analysis and Measurement with Biological Redox Systems

Studies of biological active redox systems, and their electroanalytical application typically involved some added, reversible electron transfer couples to mediate the biological couple's reaction or

electrochemical detection of a product of the reaction between the biological component and an analyte substrate.

CHAPTER THREE

MATERIALS AND METHODS

3.1. INSTRUMENTATION FOR CYCLIC VOLTAMMETRY

Cyclic voltammograms generated from the cycling of potentials within a specified potential range, were obtained using a Princeton Applied Research (PAR) model 173 Potentiostat/ Galvanostat equipped with a logarithmic current converter model 396 that controlled the current. This electrochemical system was interfaced to a PAR model 175 Universal Programmer that generated triangular waves. The output signal was fed into a PAR RE0089 X-Y recorder.

The dual function of A potentiostat/galvanostat is illustrated by the fact as a potentiostat it holds the potential between two electrodes of an electrochemical cell constant while as a galvanostat it holds the current in a controlled manner despite large changes in the applied potential required to maintain current control (Gosser, D.K 1994).

3.1.1 Mode of operation of a potentiostat

A potentiostat in general maintains constancy in potential between the working and reference electrodes. In a three-electrode open electrochemical cell the reference electrode is positioned in the proximity of the working electrode. The auxiliary (counter) electrode is the third electrode in the electrochemical cell. Since, the potential of the reference electrode is constant, the potentiostat basically senses the potential of the working electrode.

The reference-working electrode pair is connected through a circuit that draws essentially no current.

In its fundamental operation, the potentiostat is generally configured as a controller circuit instrument that responds to variations in the potential between the two electrodes through a negative feedback circuit containing the counter electrode in such a way as to reduce the difference to zero. During this operation no current is drawn through the reference electrode. In other words, the potentiostat controls the voltage across the working electrode-counter electrode pair and adjusts this voltage to maintain the potential difference between the working electrode and reference electrode. This difference is sensed through a high impedance feedback loop, in accordance with the program supplied by a function generator. Thus the adjustment is enforced by supplying whatever current is required through the counter electrode. This is the current that is experimentally recorded.

A key electronic unit which is important in the operation of the potentiostat is the operational amplifiers which control its operation. The operational amplifiers are complex electronically, but can be represented as a simple three terminal black box with several connections. The amplifiers

have two power supplies, one at +15V and the other at -15V, relative to a common circuit point defined at the power supplies called ground. Measurements are made relative to this ground which may or may not be related to the earth ground.

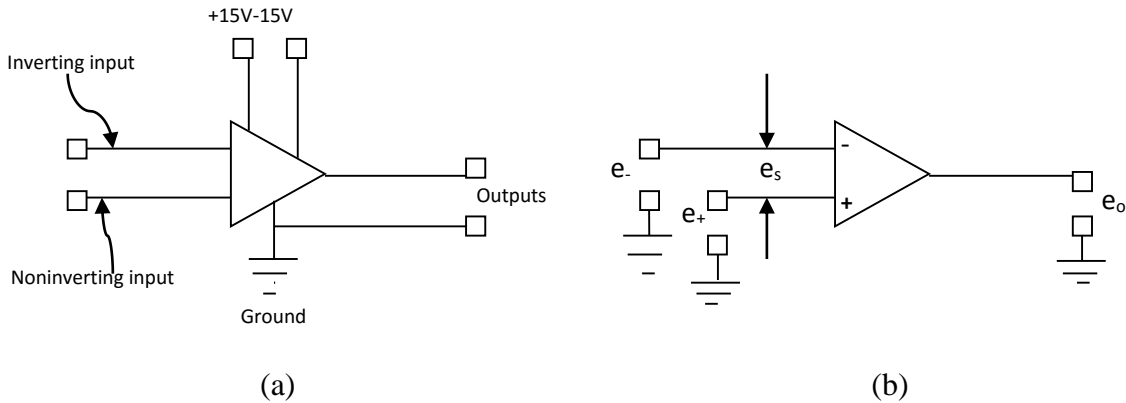


Figure 3.1. Schematic diagrams for operational amplifiers (a) shows the power connections (b) shows the way the amplifiers are usually depicted.

In an operational amplifier there are input and output connections and one side of the output is ground. In most cases neither of the input is ground hence they are both floating away from the ground.

The operational amplifier has two terminals for inputs and are referred to as the inverting (-) and noninverting inputs (+). They are characterized by an infinite input impedance, meaning they can accept an input voltage without drawing current into the device through the voltage source.

The third terminal in the operational amplifier is output, e_o or E_{out} , which has zero impedance so that the output voltage remains constant irrespective of the current drawn by the load.

The amplifier is an inverting differential amplifier with infinite gain, A , so that $E_{out} = -A(E_- - E_+)$ and any voltage difference at inputs drives the output $\pm \infty$. The fundamental property of the amplifier is that the output, e_o , is the inverted amplified voltage difference, e_s , where e_s is the voltage of the inverting input with respect to the noninverting input, i.e.

$$E_o = Ae_s \quad (1)$$

A is the open loop gain and e_s is the sum of the inverted amplified signal e_- and the non-inverted amplified signal e_+ such that the above equation becomes

$$e_o = Ae_- + Ae_+ \quad (2)$$

Since $e_s = e_- - e_+$

To use operational amplifiers as a control device there is negative feedback where some of the output voltage is fed to the inverting input of the amplifier as shown below:

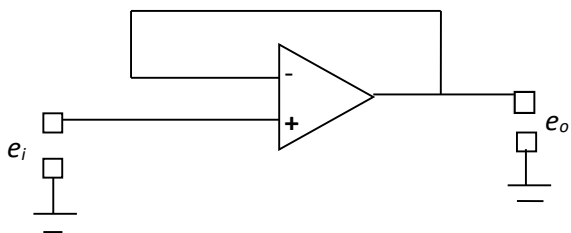


Figure 3.2. (a) A voltage amplifier

In this configuration the amplifier operates to maintain the potential difference between the inputs at zero. Any error across these inputs ($+\delta V$) is amplified to give an output ($-A\delta V$) that acts to reduce the error $+\delta V$ back to zero. This simple configuration is an extremely useful circuit known as the voltage follower because the output voltage follows exactly the input voltage. The input impedance of the device is infinite and the output impedance is zero. This means that the circuit can measure potential at its input without drawing current from the voltage source and display the result on a measuring device, which draws current.

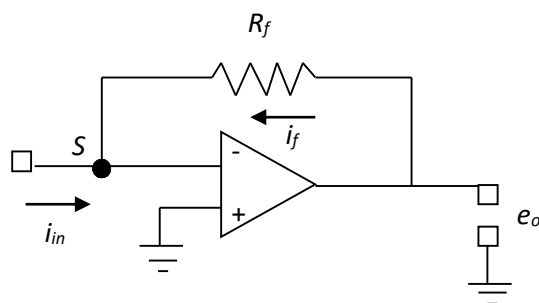


Figure 3.3. (b) A current follower

The current follower on the other hand, finds application in the measurement of the cell circuit. In the circuit shown in Figure 3.3 (b), the feedback element is the resistor, R_f , through which there is a feedback current, i_f . The input is a current, i_{in} , from a working electrode. Based on the conservation of charge the sum of all the currents into the summing point S must be zero and since negligibly a small current passes between the inputs:

$$i_f = -i_{in} \quad (3)$$

Therefore from Ohms law,

$$\frac{e_o - e_s}{R_f} = i_{in} \quad (4)$$

and by substitution from equation (1)

$$e_0 \left(1 + \frac{1}{A} \right) = i_m R_f \quad (5)$$

Since the value A is very high, the quantity in the bracket is approximately 1.00, hence

$$e_0 \cong i_m R_f \quad (6)$$

Thus the output voltage is proportional to the input current by a scale factor determined by R . The circuit is called a current follower or a current-to-voltage (i/E or i/V) converter. The voltage of the summing point e_s is $-e_0/A$, which for a typical device, lies between $\pm 15V/10^5$ or $\pm 150\mu V$ i.e., S is a virtual ground. Though it is not a true ground in that there is no direct connection it has virtually the same potential as ground, a very important feature because it allows currents to be converted to equivalent voltages while the current source is maintained at ground potential. This virtue is utilized in the building of a potentiostat.

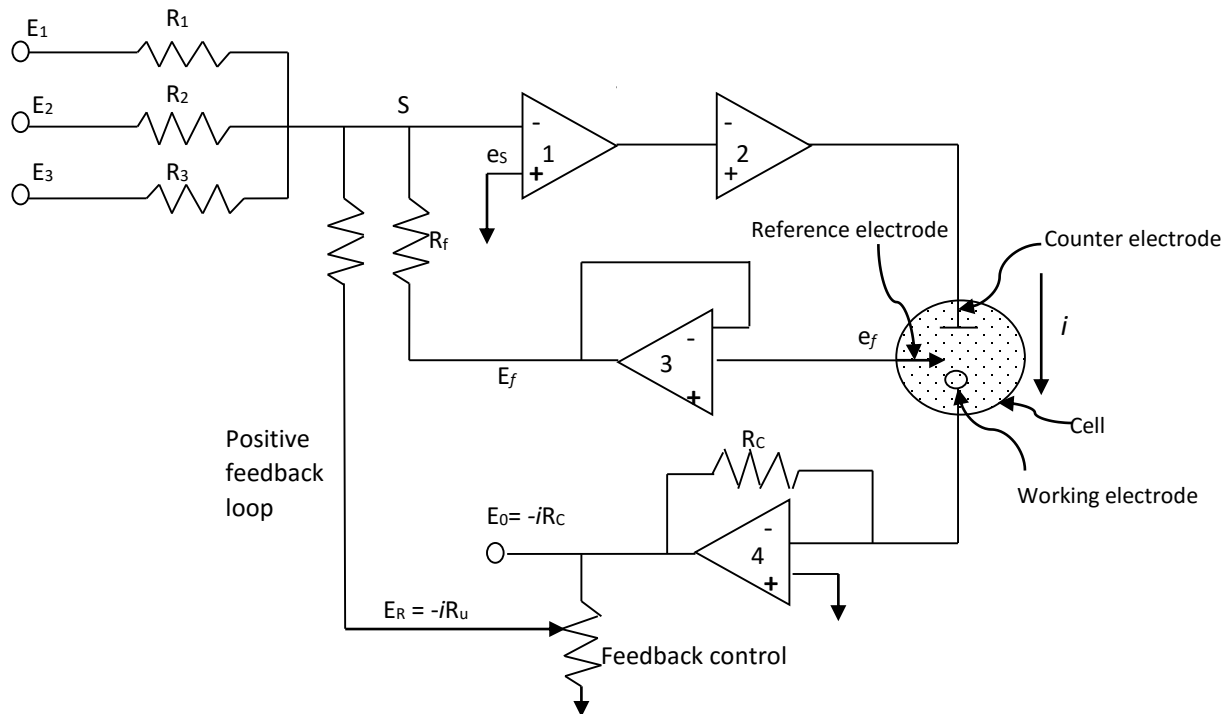


Figure 3.4. (c) A potentiostat with a positive feedback compensation.

Figure 3.4 (c) above represents a potentiostat configuration that has been most widely used. It is referred to as the “adder” configuration. It has an advantage over other configurations because all of the control inputs can be referred to the ground as well as the output voltage of the current follower (amplifier 4) which is proportional to the current. However the internal impedance of the control inputs must be low. The working electrode is maintained by amplifier 4 at virtual ground, which is a current follower configuration. The output of the amplifier 4 is given by

$$E_0 = -iR_C$$

meaning that E_0 is proportional to the current flowing through the working electrode. This means that amplifier 4 acts as a current follower and hence the current changes in the cell are monitored when its output is fed into a recorder. The operational amplifier 3 is a voltage follower such that the output E_f is equal to the input e_f . The potential e_f is the potential of the reference electrode measured with respect to the working electrode because this is the reverse of the conventional definition of the E_{cell} ,

$$E_f = e_f = -E_{\text{cell}} = -(E_{\text{working}} - E_{\text{reference}}) \quad (7)$$

This assumes that there is no uncompensated iR drop in the cell, which includes the solution, the leads to the working electrode and the working electrode itself. The voltage follower draws only minute current through the reference electrode, so that iR drops in the reference electrode are negligible. If iR drops are present in the solution or in the electrode

$$E_f = -E_{\text{cell}} + iR_u \quad (8)$$

Where R_u is the uncompensated resistance and i is the cell current. The only electrically measurable quantity here is the potential of the lead from the reference electrode measured with respect to the lead from the working electrode. At zero current this is equal to $-E_{\text{cell}}$.

The control inputs E_1 , E_2 , E_3 , and the voltage follower E_f are added and summed through separate input resistors connected to the summing point S of amplifier 1, the control amplifier. Amplifier 1 maintains its summing point at ground ($e_s = 0$) by virtue of the feedback loop that contains the counter electrode, reference electrode and follower. The term summing point refers to a current node where the algebraic sum of all the input currents is zero such that,

If $R_1 = R_2 = R_3$, then

$$-E_f = E_1 + E_2 + E_3 \quad (9)$$

From this last equation and equation (7), we have

$$E_{\text{cell}} = E_1 + E_2 + E_3 \quad (10)$$

The control amplifier forces the current to flow through the counter and working electrode to enforce the conditions described by equation (10). For example, any tendency of the summing point to drift negative with respect to ground causes the control-amplifier output and counter-electrode voltage to become more positive, E_{cell} to become more negative and E_f to become more positive, all of which tend to cancel the negative drift at the summing point.

3.1.2 Universal Programmer PAR model 175 and X-Y Recorder

The PAR model 175 universal programmer is a waveform generator with two operating modes SWEEP and PULSE. Single cycle or continuous cycle outputs can be obtained in both modes. Potential controls allow up to four inflection points to be set for a single output waveform. There is a provision for synchronizing, starting, stopping and reversing a programmed waveform. It has adjustable scan rates from 1 mV to 10^4 V/s.

In all the analysis carried in this work, the model 175 universal programmer was used in the SWEEP mode, with each of the potential set points independently adjusted over a range of ± 10 V.

The signal output from the PAR model 173 potentiostat/galvanostat and PAR model 175 programmer was fed into the recorder model RE0089 X-Y to display the voltammogram. The signal output from the PAR model 175 programmer is that one which is originally programmed (set) in the equipment.

3.2 ELECTRODE ASSEMBLY

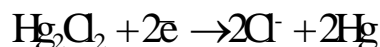
A three-electrode assembly in an undivided/open cell was used throughout this work. These consisted of a saturated calomel electrode (SCE) as the reference electrode, platinum wire as the auxiliary or counter electrode and carbon graphite, with a surface area of 0.38 cm^2 as the working electrode. The counter or auxiliary electrode was platinum wire.

The carbon graphite working electrode was supported by a 15 cm glass tube sealed on one side but having a contact wire passing through. This contact wire and the electrode were connected by means of mercury metal.

3.2.1 Reference electrode

The reference electrode used in this work was the saturated calomel electrode (SCE), this choice was based on experimental convenience. It can be prepared easily and can be used for a long time.

Its half-cell is represented as $\text{Hg}|\text{Hg}_2\text{Cl}_2|\text{KCl}(\text{sat'd})$. The potential of the SCE is 0.242 V at 298K relative to the Standard hydrogen electrode (SHE). The half-cell reaction in the SCE is given by this equation:



So $E_{(\text{SCE})} = E_{\text{Hg}_2\text{Cl}_2, \text{Hg}}$. From this redox reaction, the Nernst equation for the SCE is

$$E_{\text{Hg}_2\text{Cl}_2, \text{Hg}} = E^0_{\text{Hg}_2\text{Cl}_2, \text{Hg}} + \frac{RT}{2F} \ln \left(\frac{a_{(\text{Hg}_2\text{Cl}_2)}}{a_{(\text{Hg})}^2 a_{(\text{Cl}^-)}^2} \right)$$

Mercury and calomel are pure substances, so their activities are unity. If the activity of the chloride ion is maintained at a constant level, then $E_{(SCE)}$ will have a constant value, which explains why the couple forms the basis of a reference electrode.

At the 'heart' of the SCE is a paste of liquid mercury and mercurous chloride (Hg_2Cl_2), which has the old-fashioned name 'calomel'. Figure below depicts a simple representation of the SCE.

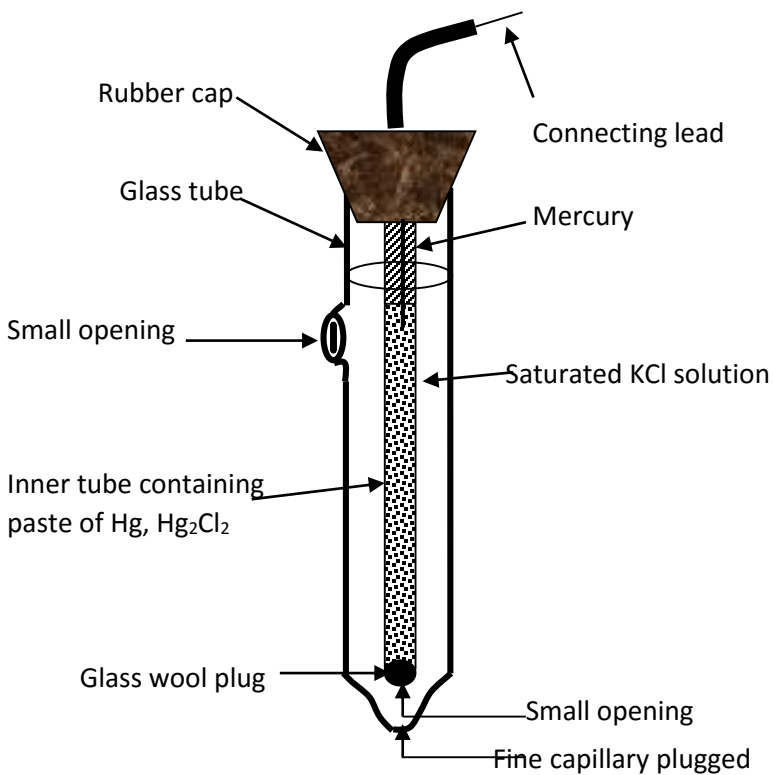


Figure 3.5 Saturated calomel electrode (SCE)

3.4 SAMPLE PREPARATION

The Hydrocortisone, Top-lemon and Extra Clair were used as received without further purification. The carbon graphite working electrode was dip coated with the modification cream and the slurry on the surface was smeared giving a uniform spread on the carbon graphite working electrode surface.

To prepare bentonite modified electrode we placed a small amount of this clay on a clean tile, then electron-inactive adhesive (Henkel) was added and mixed with it thoroughly until a thick slurry was obtained. The slurry was smeared uniformly on a smooth surface of a freshly prepared carbon electrode. The electrode was left to dry at room temperature for 24 hours; as a result we obtained dry bentonite on the surface of the electrode.

Composite mixtures for preparing composite electrodes involved mixing the substances in the required ratios on a weight/weight basis. This mixture was smeared uniformly on the working electrode surface as already discussed.

Polyaniline, was prepared by electrodepositing polyaniline on a freshly polished bare carbon electrode by cycling the potential from -0.2V to 0.80V in a solution containing 0.1M aniline and 1M H₂SO₄. This is the optimum electrolyte composition for electrodepositing aniline. The scan rate was set at 20 mV/s while the current scale was at 10 mA/V. The sensitivity of the recorder was set at 50 mV/cm.

3.5 CHEMICAL REAGENTS

The Hydrocortisone medicated cream, Top-lemon and Extra Clair beauty creams were used as received without further purification.

The monomer liquid aniline (Aldrich, 98%), was triply distilled until a colorless liquid was obtained. It was then stored under an inert gas nitrogen. This distillation process was repeated for each fresh experiment. All the chemicals and acids were analytical grade and were used as namely sulphuric acid (Gowa), and hydrochloric acid (Gowa). Other chemicals used include acetonitrile, sodium chloride (sigma), and p-aminophenol (BDH)

All solutions were prepared using high purity solvents. Distilled water was obtained from a Millipore water purification system. For the non-aqueous studies, acetonitrile (HPLC grade, Fischer) was used as received.

All weighing's were done using an analytical balance for maximum accuracy.

The bentonite (Athi River Mining Company Ltd., Kenya) has a mesh size ranging from 150 to 200 μm , cation exchange capacity (CEC) 1.18 – 1.22 mM/g and pH range of 8.4 – 9.6. The density of bentonite is 1.25 g/cm^3 which are comparable to other clay minerals from different parts of the world (Rask, 1984). It has average solvent retention capacity of 22.5% and 4.8% for water and organic solvents respectively. Its moisture content is 8.5%. It swells by a factor of 1.7 and 1.4 in water and organic solvents respectively.

It was purified as described by other researchers (Gosh and Bard, 1983, and by Egeet.al., 1984)

The elemental composition of the raw bentonite (main elements) as determined by XRF analysis is shown in the Table below (Orate and Segar, 1999)

Table 3.1. Elemental composition of raw bentonite.

ELEMENT	CONCENTRATION ($\times 10^{-3}$ g/g)
Mn	8.35
Ca	37.0
Na	10.855
K	8.35
Pb	0.021
Cr	0.068
Al	171.1
Ti	8.10
Zn	0.096
Mg	16.5
Ni	0.016
Cu	0.069
Sr	0.313
V	8.10
Zr	3.776

P ₂ O ₅	0.569
Ba	3.776
SiO ₂	469.71
Rb	0.069
Fe	50.5

3.6 GLASSWARE

The glassware was cleaned by soaking them in HNO₃ and H₂SO₄ mixtures for several hours. They were then cleaned using detergent, ordinary water and finally rinsed with triply distilled water. They were then dried in the oven before use.

CHAPTER FOUR

RESULTS AND DISCUSSIONS

4.1 ELECTROCHEMICAL STUDIES ON TOP LEMON- BEAUTY CREAM

Top lemon is a popular beauty cream used extensively in Kenya due to its skin lightening properties. Unfortunately, top lemon, despite its wide circulation in the Kenyan market and the fact that it can be easily bought or accessed from counters in pharmacies, chemists and beauty shops is not approved by the Kenya Bureau of Standards (KEBS). This assertion is based on the fact that the product does not bear the diamond quality mark of KEBS. Because of its skin lightening properties, it is easy to speculate that it either contains mercury or hydroquinone as a constituent. In this work, surface modified electrode technique was used to study this cream and verify the existence of the any of the chemicals mentioned.

4.1.1 Modification of Carbon Graphite Working Electrode with Top Lemon Cream

The carbon graphite working electrode was polished as already discussed elsewhere giving a glossy finish. The top lemon cream was applied on the carbon graphite working electrode giving a thin layer with a uniform surface as was the case with hydrocortisone. This electrode was then put in an electrolyte solution containing 1M Sulphuric acid. The potential of the working electrode was cycled from -0.3V to 0.9V at a scan rate of 20mv/s. The cyclic voltammetric response showed well defined oxidation peaks occurring at 0.61V and a reduction peak occurring at 0.21V. See Figure 4.1.

It is proposed that this redox process represents the Quinone/imine redox process. This redox peaks resembles that observed when polyaniline is oxidized at far positive potentials leading to its degradation yielding Quinone/imine derivatives.

This explanation has been captured conclusively in the polyaniline oxidation state scheme discussed in the introduction chapter.

The total oxidative and reductive charges were computed. The values obtained were 8×10^{-6} coulombs /cm². The values obtained indicate that the oxidative and reductive charges are nearly equal indicating the process is reversible and has excellent faradaic characteristics for the redox process. The surface coverage Γ for the oxidative process was computed from the equation

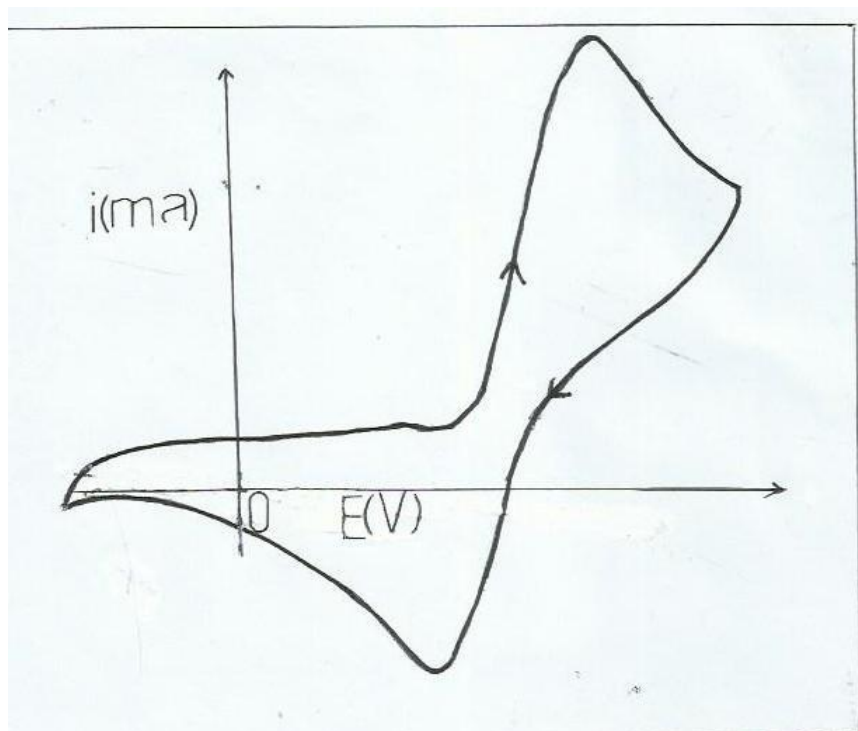


Figure 4.1: Cyclic voltammogram for Top-lemon modified electrode in 1.0M H₂SO₄ at a scan rate of 20mV/s. Potential range: -0.3V to 0.9V. **CV Scale:** 0.09V/cm (x-axis): 0.02mA/cm (y-axis)

$$\Gamma = \frac{Q_{\Delta x_i}}{nFA}$$

Where Q_{ox} is the oxidative charge, n is the number of moles of electrons, F is the Faraday constant and A is the surface area of the electrode. The value obtained was.....moles/cm²; this value is the quantity of the Quinone derivative in the cream. It is possible that there could be slight differences with the actual amount of Quinone obtained gravimetrically. The top lemon modified electrode was then subjected to scan rate dependence studies. A plot of oxidative peak current versus square root of scan rate yielded a linear plot suggesting the process

is diffusion limited.

The effect of pH was studied by cycling the potential of the Top lemon

modified electrode from -0.3V to 0.90V at scan rate of 10mv/sec in electrolyte solutions containing 0.125M, 0.25M, 0.50M, 1M and 2M H₂SO₄. The resultant cyclic voltammogram is as shown in Figure 4.2.

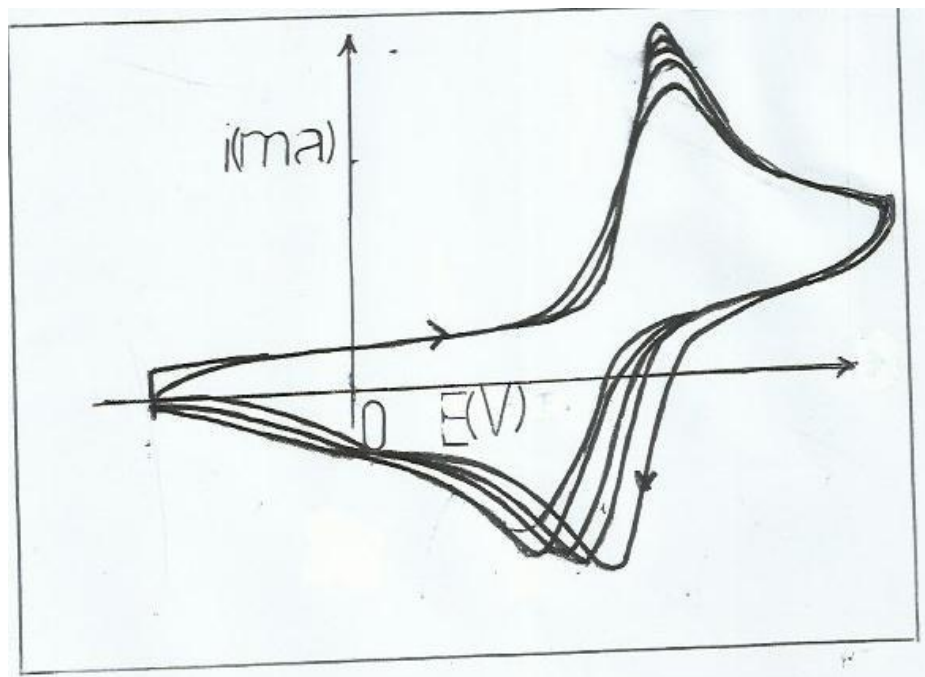


Figure 4.2: Effect of solution pH on the Top-lemon redox process. Potential range: -0.30V to 0.90V. Scan rate 20mV/s. **CV Scale:** 0.09V/cm (x-axis): 0.02mA/cm (y-axis)

An extensive shift in the reductive peak potentials towards positive potentials is observed as the pH is lowered as shown in the Table below.

Table 4.1: Effect of pH on the redox potentials

E_{red}	pH
0.14	0.90
0.16	0.60
0.19	0.30

0.22	0.0
0.25	-0.30

The change in reduction potential versus pH i.e., $\frac{\Delta E_{\text{red}}}{\text{pH}}$ is approximately 120mv/pH. This confirms that this process is $a2\text{H}^+/\bar{e}$ or $2\text{H}^+/2e$, which is in agreement with the Quinone/imine process (Orata and Buttry, 1987)

4.2.2 Top lemon modified carbon graphite electrode in Sodium Chloride supporting electrolyte.

The supporting electrolyte was now changed to 1M NaCl, and the potential of the Top lemon modified carbon-graphite electrode cycled from -0.30V to -0.90V at a scan rate of 10mv/s. The cyclic voltammetric response shows an oxidation peak at 0.13V and 0.58V (as shown in Figure 4.3)

There is a single reduction peak at -0.01V. There is a significant difference in the redox response of the Top lemon modified carbon graphite electrode in NaCl supporting electrolyte as compared to the case of sulphuric acid supporting electrolyte discussed previously. These differences can be attributed to the difference in the cations and anions of the supporting electrolyte, which are always known to ingress or egress out redox systems. The ingress or egress of ions will be influenced by for example the charge densities of the ions which depends on the ionic radii, ion mobility and the charge i.e. charge density of the chloride is higher than that of Hydrogen sulphate (HSO_4^-) or sulphate (SO_4^{2-}). The cations, sodium ions (Na^+) and hydrogen ions (H^+), though belonging to the same group in the periodic table, also have significant difference in the ionic radii and mobility. It is therefore proposed that, the charge density and the ionic radii, definitely affect the redox process and this is reflected in the redox potentials.

The potential window of the Top lemon modified carbon-graphite electrode was then varied from -0.30V to 0.70V, 0.75V, 0.80V, 0.85V and 0.90V. It is observed that there was no change in the oxidation/reduction peak potentials. This observation is a veiled pointer to the stability of the redox center/sites in the Top lemon.

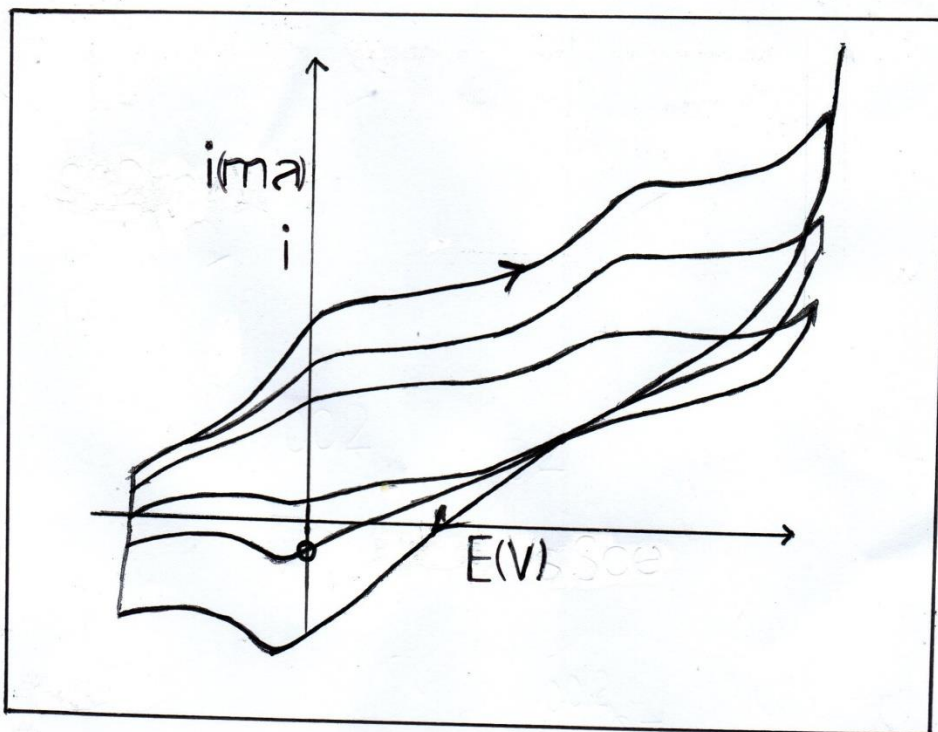


Figure 4.3: The cyclic voltammetric response of Top lemon electrode in 1M NaCl. Potential range: -0.30V to 0.90V, scan rate of 10mV/s. **CV Scale:** 0.09V/cm (x-axis): 0.02mA/cm (y-axis)

4.1.2 Top Lemon on Polyaniline modified carbon graphite electrode

The supporting electrolyte was now changed to 1M NaCl. The Top lemon on a polyaniline modified carbon-graphite electrode had its potential cycled from -0.30V to 0.90V and the scan rate varied from 10mv/s, 20mv/s, 50mV/s and 100mv/s. The resultant cyclic voltammogram is shown in Figure 4.4.

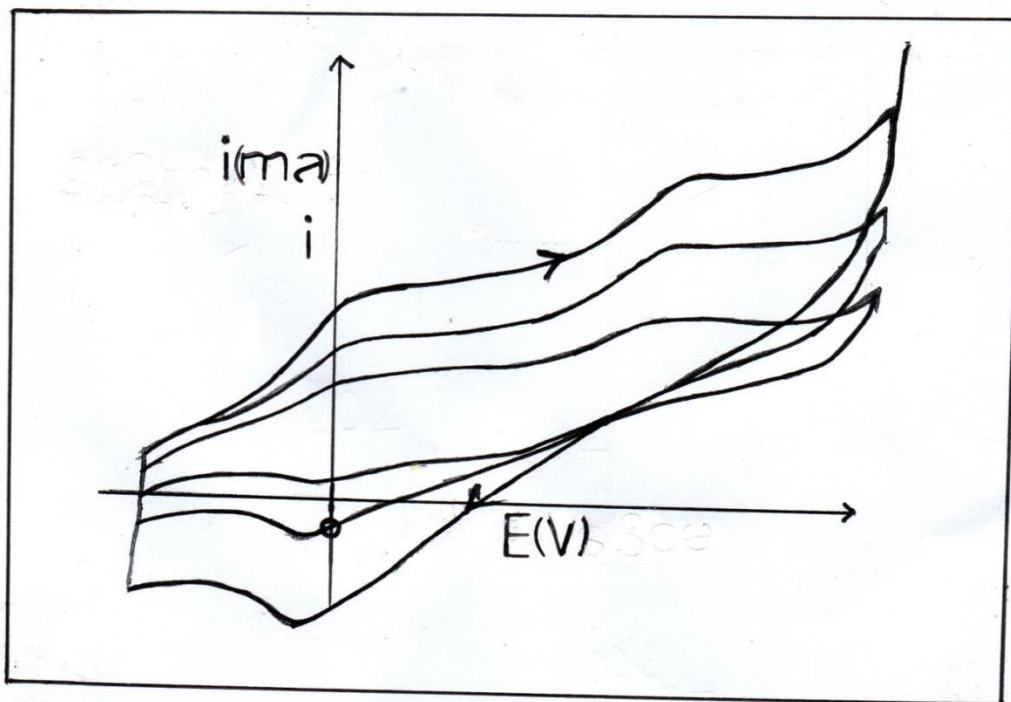


Figure 4.4: Cyclic voltammogram for Top-lemon on polyaniline modified electrode in 1M NaCl. Scan rates-10mV/s, 20mV/s, 50mV/s and 100mV/s. Potential range: -0.30V to 0.90V. **CV Scale:** 0.09V/cm (x-axis): 0.02mA/cm (y-axis)

It is observed that there are two oxidation peaks occurring at approximately 0.33V and 0.57V at a scan rate of 5mV/s. As the scan rate is increased, the oxidation peak potentials shift by approximately 100mV. On the other hand, there is only one reduction peak which occurs at 0.42V, at a scan rate of 5mV/s. Similarly, on varying the scan rate, the reduction peak shift towards negative potentials by approximately 100mV. This is not the same for

the oxidation peak potential, which shifted positively as the scan rate was increased. Since variation of scan rate gives insight into the kinetics of the redox process, these shifts are therefore a veiled pointer to the time dependent changes in the nature of the redox sites resulting from a combination of entropic effects and the intrinsic nature of the redox species.

A plot of the anodic peak current, versus square root of scan rate, yielded linear plots with a correlation coefficient of 0.98. This implies that the process is diffusion limited as expected. When the potential window of the Top lemon modified electrode was varied from -0.30V to 0.70V,

0.75V, 0.80V, 0.85V and 0.90V at a scan rate of 10mV/s, it is observed that there is no change/variation in the oxidation/reduction peak potentials. This can be attributed to the stability of the redox centers.

4.1.3 Top lemon on Polyaniline Modified Electrode

Polyaniline was once again electrodeposited on the carbon graphite electrode by cycling the potential of the carbon-graphite electrode from -0.30V to 0.90V, at a scan rate of 20mV/s in a solution containing 0.1M Aniline and 1.0M Sulphuric Acid. The resultant cyclic voltammogram for the polyaniline redox process is shown in Figure 4.5 below.

The polyaniline modified electrode was then modified with Top lemon by dip coating as discussed in the experimental and methodology section. . This electrode was then put in a solution containing 1M Sulphuric Acid and 0.1M aniline. The potential was cycled from -0.30V to 0.90V at a scan rate of 10mv/s. It is observed that the oxidation/reduction peak potentials for polyaniline occurs at 0.31V and 0.04V respectively, while the quinonic peaks associated with polyaniline appear at 0.53V and 0.40V respectively for the oxidation-reduction peaks.

It was expected that; when the polyaniline electrode was modified with Top Lemon, and the potential cycled in the electrolyte solution, containing aniline, polyaniline will continue being electrodeposited. This was not the case instead, an oxidation peak and a broad reduction peak are occur at 0.39V and 0.15V respectively.

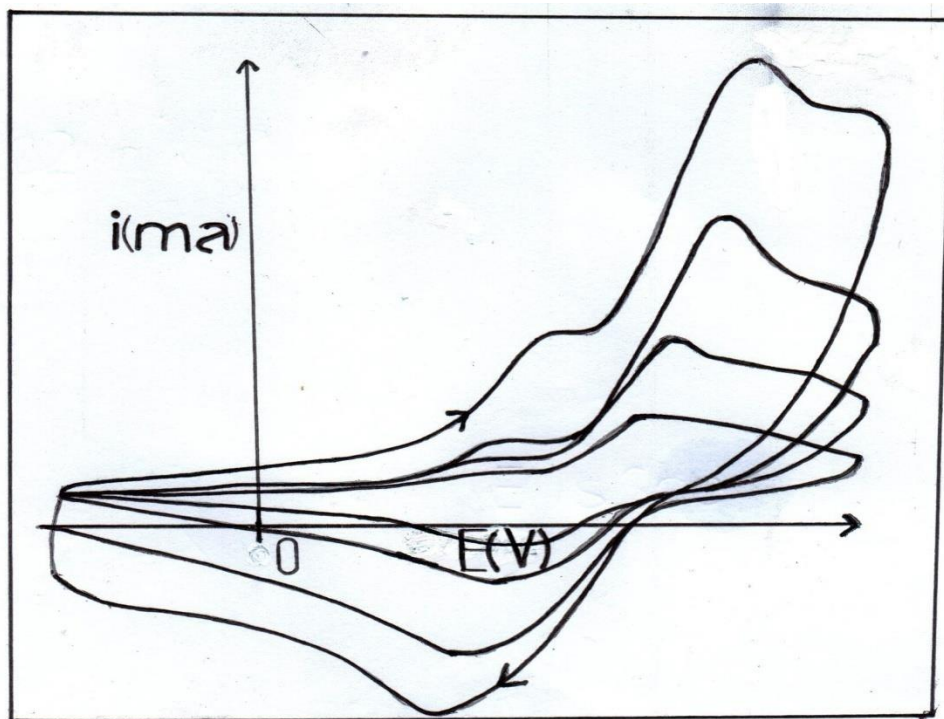


Figure 4.5: Electrodeposition of polyaniline on carbon graphite electrode. Potential cycled from -0.30 V to 0.85 V, scan rate 20mV/s. **CV Scale:** 0.09V/cm (x-axis): 0.02mA/cm (y-axis)

These results, when compared to the case of Top Lemon on bare carbon graphite, where oxidation and reduction peaks for the Top-lemon redox process occurred at 0.60V and 0.21V respectively, suggest that there was a significant alteration in both the polyaniline and top lemon redox processes. It is proposed that the redox profile observed in Figure 4.6 can be attributed to the formation of a composite structure, where the redox centers of polyaniline and Top Lemon interact substantively. This assertion is based on the fact that if the structure was a bi-layer, then

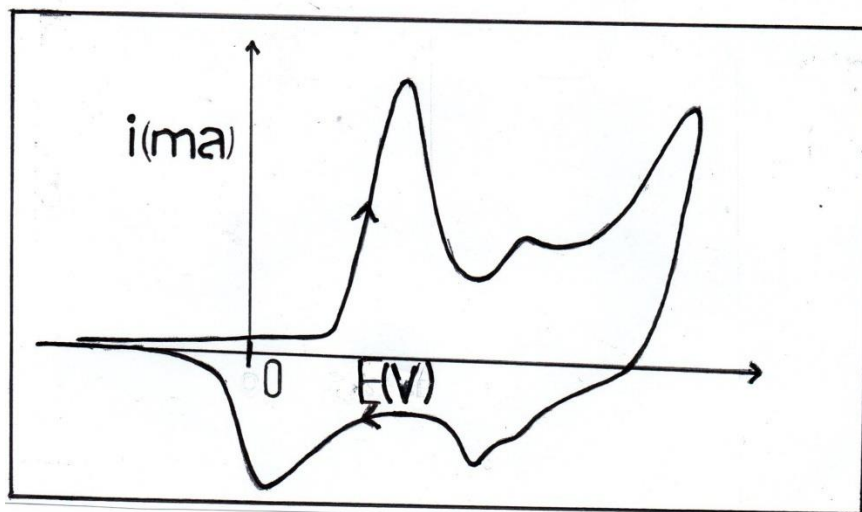


Figure 4.6: Cyclic voltammetric response for Top lemon on polyaniline modified electrode in 1M sulphuric acid and 0.1M aniline. Scan rate 20mV/s. **CV Scale:** 0.09V/cm (x-axis): 0.02mA/cm (y-axis)

the polyaniline and Top lemon redox processes would have been independent of one another, /and or redox junctions characterized by charge rectification would have been observed.

Fresh polyaniline electrode was electro generated and further modified with Top lemon. This electrode was then transferred to various supporting electrolytes containing 0.1M, 0.25M, 0.5M, 1.0M and 2M Sulphuric acids (H_2SO_4). It is observed that as the H^+ ion concentration is increased, the redox profile/faradaic process improved leading to well defined reduction peaks. This improvement in the reduction peak profile as the concentration of Hydrogen ions (H^+) is increased mathematically mimics a homogenous function of 1st degree, where the factor (α) and the thermodynamic function M is the potential of the redox center. This potential is related to the Gibbs function ($\Delta G = -nFE$). Therefore, applying the Euler Theorem;

$$\alpha nM = \sum_i n M$$

Where n is the concentration of the redox centers, and M is the Gibb's free energy , a function of the redox potential, hence; correlates to the population of the redox centers. Further refinement yield

$$[H^+]nM = \sum_i n M$$

$$[H^+]M = \sum_i \frac{n}{n} M = \sum_i x M$$

$$M = \frac{1}{[H^+]} \sum_i x M$$

Where, (α) is $[H^+]$ and x is the mole fraction of the identical redox centers, hence;

$$M = \frac{1}{[H^+]} \sum_i x \left(\frac{\partial M}{\partial n} \right)$$

Therefore, for the individual identical redox centers; 1,2,3.....etc.

$$M = \frac{1}{[H^+]} \left\{ x \left(\frac{\partial M}{\partial n} \right) + x \left(\frac{\partial M}{\partial n} \right) + x \left(\frac{\partial M}{\partial n} \right) + \dots \right\}$$

Note that, the M (Gibbs function) is proportional to the redox potential. It is also important to note that, it is assumed that the effect of $[H^+]$ on the faradaic processes is linear. Similarly, the redox potential is assumed to be an average of the potentials of the many individual redox centers, i.e., bulk property.

The Top Lemon on PANI modified electrode had its potential cycled from -0.30V to 0.90V in a solution containing 0.1 aniline and 1.0M Suphuric acid. The electrode was subjected to scan rate dependence studies, a plot of anodic peak current versus scan rate yielded a linear plot suggesting that, the Top Lemon is surface attached. This observation brings to light the influence of the polyaniline host matrix on the surface properties of Top Lemon. This is confirmed by the fact that, when Top Lemon is attached on bare carbon-graphite electrode, the redox process is diffusion-limited, whereas on the polyaniline modified electrode, its redox process is not diffusion-limited. It is therefore proposed that the linear plot obtained for the peak current versus scan rate, which suggests that Top Lemon is surface attached, is an indication that there is electrostatic interaction between the Top Lemon redox sites with those of polyaniline when the polymer is switched from the insulating to the conducting state.

This is further confirmed by the resultant redox peaks observed in the cyclic voltammogram, which displayed composite properties for both the polyaniline and Top Lemon. The composite oxidation and reduction potential occurred at 0.31V and 0.13V respectively.

When the Top lemon on polyaniline modified carbon-graphite electrode had its potential cycled from a constant 0.30V to varying positive potential limits (0.70V, 0.75V, 0.80V, 0.85V and 0.90V)

in a solution containing 0.5M sulphuric acid. The broad and misshapened oxidation-reduction peaks obtained did not show any change in the potentials, nor incremental increments in the oxidation and reduction peak currents (Figure 4.7), implying the redox process has low efficiency.

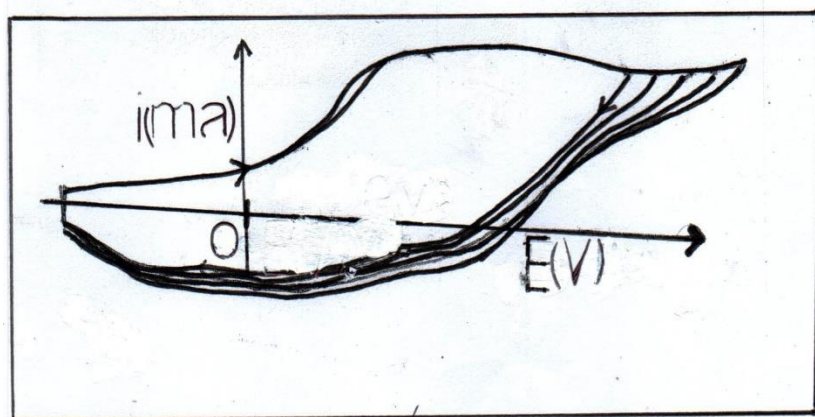


Figure 4.7: Effect of variation of positive potential limit on Top-lemon redox process. Potential range: -0.3V to 0.90V, scan rate 20mV/s. **CV Scale:** 0.09V/cm (x-axis) : 0.02mA/cm (y-axis)

It is important to note that traditionally, PANI, when cycled to far positive potentials in acid solution, in the absence of aniline monomers electro-degrades to form Quinone-imine derivatives (Orata et al., 1997)

In this case, there was no evidence of electro-degradation of polyaniline despite being the host matrix. Therefore, it is possible that the presence of the Top Lemon inhibits or significantly reduces the oxidative stress in polyaniline hence slowing down the electro-degradation process.

A fresh Top lemon on polyaniline modified carbon-graphite electrode was prepared and transferred to a solution containing 1.0M HCl and the potential was cycled from -0.30V, to 0.75V at varying scan rates. The resultant cyclic voltammetric response yielded broad and misshapened peaks as shown in Figure 4.8, with the oxidation and reduction peak potentials estimated to occur at 0.44V and 0.30V

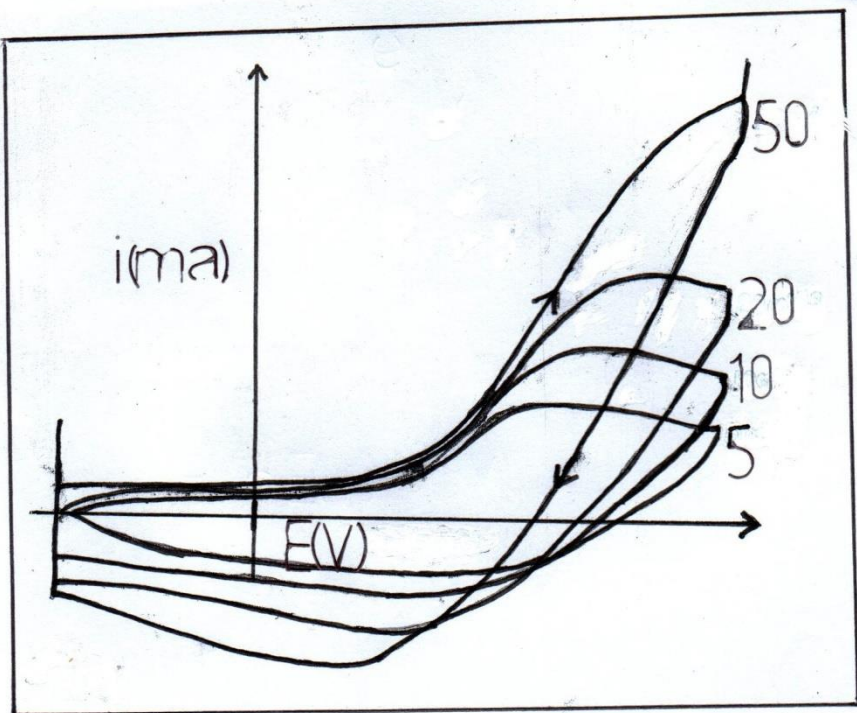


Figure 4.9: Cyclic voltammetric response for Top-lemon on polyaniline modified electrode in electrolyte solutions containing 1.0M HCl at varying scan rates-5mV/s, 10mV/s, 20mV/s and 50mV/s. **CV Scale:** 0.09V/cm (x-axis) : 0.02mA/cm (y-axis)

The broad and misshapened peaks are typical of slow electron transfer kinetics/and or interference with the electron transfer dynamics. This is most likely the result of the activity of chloride ions (Cl^-). It is known that chloride ions have a high charge density given their small ionic radii and can therefore disrupt the individual redox processes in PANI and Top lemon. This interference results from ingress and egress of chloride ions into the PANI and Top lemon matrix.

Increasing the positive potential limit for the Top lemon on polyaniline modified carbon graphite electrode in the HCl supporting electrolyte, did not lead to electro-degradation of polyaniline. This again has already discussed is probably the result of inhibitory or suppressive tendencies of Top-lemon on the polyaniline redox process. This is expected based on Le Chatelier's principle, since Top lemon has hydroquinone, therefore production of Quinone/ imine derivatives at far positive potential by polyaniline during electro-degradation will be suppressed.

4.1.4 Effect of p-aminophenol on Top-lemon redox process on different host matrices

Bare carbon graphite working electrode was modified with Top-lemon cream as already described earlier in this study. The Top lemon derivatised electrode was then transferred to a solution containing 0.01M p-aminophenol and 1.0M HCl. The potential of the electrode was cycled from -0.30V to 0.90V at a scan rate of 20mv/s. The resultant cyclic voltammogram had a broad oxidation peak occurring at approximately 0.73V and a reduction peak at 0.48V. When the scan rate is varied, an equivalent of an isoelectric point or a node which is typical of metal redox processes is observed at 0.64V (see Figure 4.10). This isoelectric points/or nodes typify nucleation processes. It is apparent that the presence of p-aminophenol does not reduce the oxidative stress or electrocatalyse the Top Lemon redox process. It is observed that the oxidation peak potential is increased by 120mv and the reduction potential by 270mv towards positive potentials. The isoelectric point/node observed at 0.64V with increasing scan rate, suggest the presence of equivalent redox sites resulting from nucleation process in the system. It is further proposed that these redox centers are in equilibria with the net change in Gibbs' free energy being zero ($\Delta G=0$).

When the solution pH is varied i.e., 0.1M HCl, 0.5M HCl and 1.0M HCl, the cyclic voltammetric profile changes as expected with broad misshaped peaks typical of slow electrode kinetics being observed at high pH. This is expected due to changes in the proton population, hence affecting the protonation-deprotonation equilibria.

In the next set of experiments, the carbon-graphite working electrode was modified with polyaniline by cycling the potential from -0.2V to 0.85V at a scan rate of 20mV/s in a solution containing 0.1M aniline and 1.0M sulphuric acid. This PANI electrode was then modified with Top Lemon as already discussed earlier in the study. The electrode was then transferred to a solution containing 0.5M HCl and 0.01M p-aminophenol.

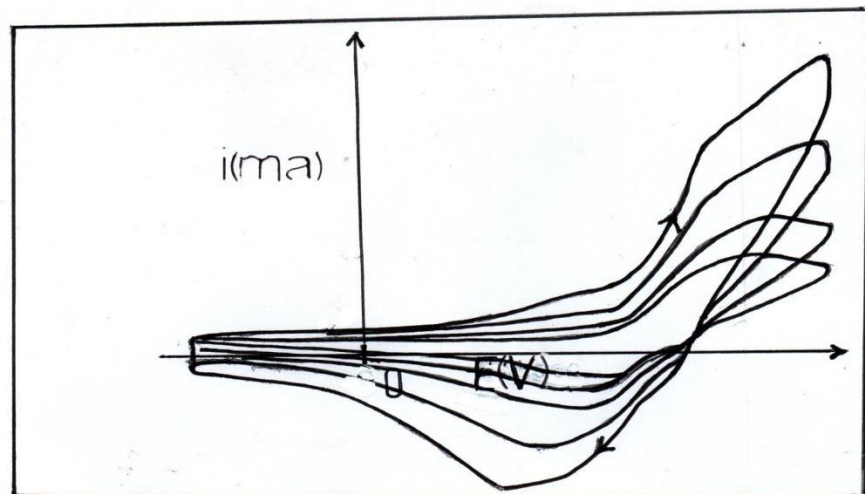


Figure 4.10: Top-lemon modified electrode in solution containing 0.01M p-aminophenol and 1M HCl. Potential cycled from -0.30V to 0.90V. Scan rate of 20mV/s

Oxidation peaks are observed at 0.33V and 0.66V. A broad reduction peak is observed at approximately 0.49V. This profile is in sharp contrast to the sharp well defined peaks observed in the absence of p-aminophenol.

It is apparent that the redox centers of polyaniline, Top lemon and p-aminophenol interact, with the resultant composite redox leading to the many redox shoulders observed, therefore making it difficult to attribute the peaks to a particular redox species.

Fresh carbon-graphite electrode was modified with a paste/slurry consisting of p-aminophenol and top lemon in equal amounts by weight (w/w). The electrode was then transferred to a solution containing 1M H₂SO₄ and the potential cycled from -0.30V to 0.90V at varying scan rates (5mV/s, 10mV/s, 20mV/s, 50mV/s and 100mV/s). The resultant cyclic voltammogram is shown in Figure 4.10 below.

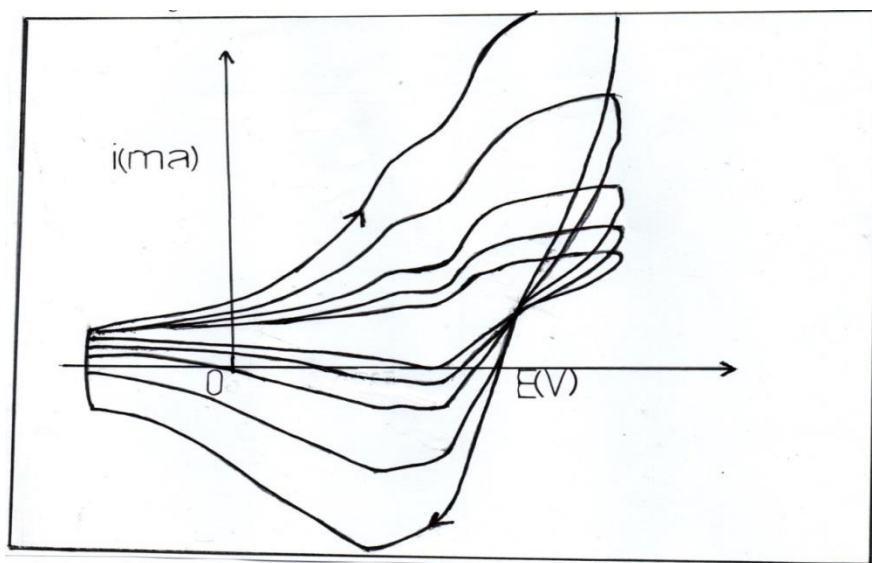


Figure 4.10: Cyclic voltammetric response for p-aminophenol-Top lemon modified electrode in 1M sulphuric acid. Potential range -0.30V to 0.90V. Scan rate 20mV/s **CV Scale:** 0.09V/cm (x-axis): 0.02mA/cm (y-axis)

It shows suppressed redox activities as compared to the case where the carbon graphite working electrode had been modified with top lemon and the potential cycled in an electrolyte solution containing 1.0M H_2SO_4 and 0.01M p-aminophenol. This observation suggests that there is a possibility of a chemical reaction between the top lemon and p-aminophenol in the slurry. This is informed by the fact that a reaction between hydroquinone and p-aminophenol can lead to the formation of an ether with aniline and phenolic groups as substituents or form an amide derivative with the proton in the amine replaced with a phenolic group, hence suppressing the intrinsic redox properties of the component substances.

4.1.5 Top lemon redox activity on a Bentonite Modified Electrode

The carbon-graphite electrode was modified with bentonite as already discussed in the previous sections. The bentonite modified electrode was further modified with Top lemon and the potential cycled from -0.2V to 0.85V at a scan rate of 20mV/s in 1.0M H_2SO_4 supporting electrolyte solution. The resultant cyclic voltammogram is as shown in Figure 4.15.

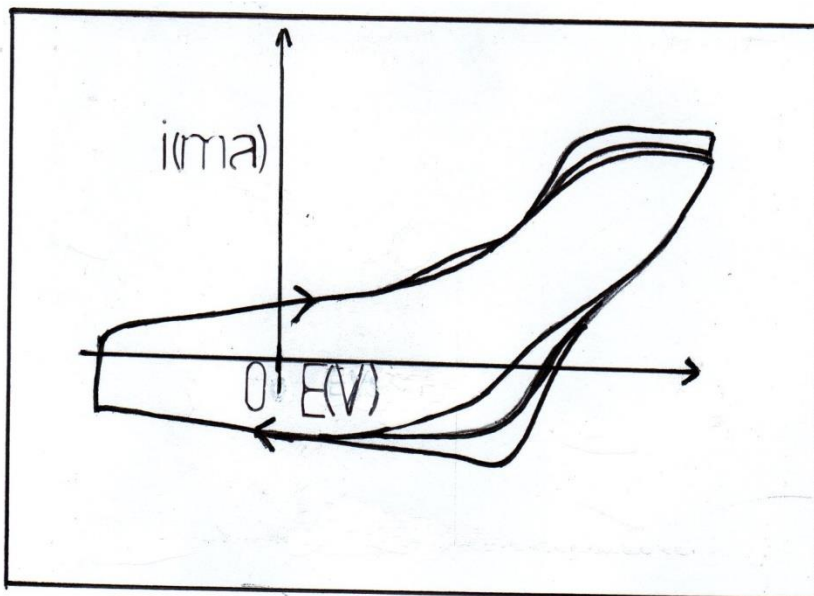


Figure 4.11: Cyclic voltammogram for Top lemon on bentonite modified electrode. Potential range: -0.20V to 0.85V. Scan rate 20mV/s

There is an oxidation peak at 0.58V and a broad reduction peak at 0.28V. The oxidation and reduction peak potentials vary with scan rate, suggesting a time dependent redox process. This suggests instability of the top lemon on the bentonite host matrix. A plot of anodic peak current versus the square root of scan rate is linear, suggesting that the process is diffusion-limited.

4.1.6. Top lemon-bentonite composite modified electrode

A fresh carbon-graphite working electrode was modified with a composite mixture of top lemon and bentonite. The electrode potential was cycled from -0.2V to -0.85V at a scan rate of 20mV/s in an electrolyte solution containing varying concentrations of H_2SO_4 (0.1M, 0.5M and 1.0M). A broad oxidation peak in all the concentrations was observed at 0.33V while the reduction peak potentials were observed at 0.37V, 0.39V and 0.42V for electrolyte solutions containing 0.1M, 0.5M and 1.0M Sulphuric acid respectively. See Figure 4.12

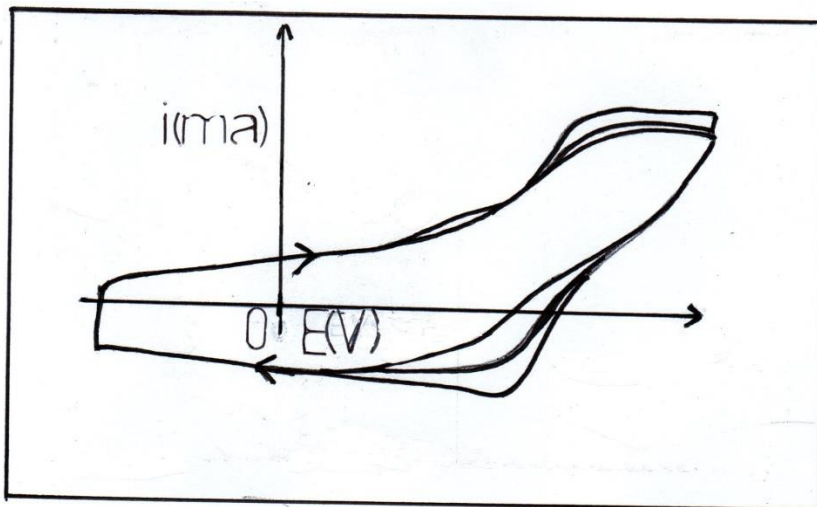


Figure 4.16: Cyclic voltammetric response for Top lemon-bentonite composite electrode in 0.1M, 0.5M and 1.0M H_2SO_4 acid. Potential range -0.2V to 0.85V, scan rate 20mV/s. **CV Scale:** 0.09V/cm (x-axis): 0.02mA/cm (y-axis)

It is apparent that, while the oxidation process is independent of pH, the reduction peak potentials shift positively, as the pH is lowered. The pH dependence of the reduction process suggest the importance of protonation -deprotonation equilibria in the process. It is also possible that the solvent population is affected as seen in the enhancement of the peak current as the pH is lowered.

The suppressed redox activities of the top lemon in the bentonite-top lemon composite is expected since the bentonite is a well-structured clay montmorillonite with tetrahedral and octahedral sites, hence the top lemon redox moieties can be structurally restricted or hindered in the matrix, affecting its redox response.

A fresh bentonite modified carbon graphite electrode was further modified by electrodeposition of polyaniline. This electrode was then modified with top lemon. The electrode was then transferred to a solution containing 1M H_2SO_4 and the potential cycled from -0.2V to varying positive potential limits, (0.70V, 0.75V, 0.80V, 0.85V and 0.90V). The resultant cyclic voltammogram is characterized by a broad oxidation shoulder at approximately 0.34V and a broad reduction band consisting of several peaks at approximately 0.03V and 0.296V.

It is obvious that the change in the top lemon redox profile by elimination is attributed to the polyaniline matrix. Since the polyaniline has an elaborate redox system and can be switched on from an insulator to a conductor, this definitely affects the top lemon-redox process. In addition, the presence of polyaniline as a composite formation with the bentonite affects the bentonite i.e., reduces the bentonite structural restrictions on top lemon as discussed earlier.

4.2 EXTRA CLAIR CREAM

4.2.1 Electro-analysis of the Redox Properties of Extra Clair Cream

Extra Clair is one of the most popular beauty creams sold in Kenyan shops. This cream has clear markings that it contains hydroquinone and despite the absence of Kenya Bureau of Standards' certification mark (Diamond quality mark) it is sold in the broader market.

Electrochemical analysis was conducted on this beauty product using surface modified electrode to confirm the existence of hydroquinone as a constituent of the cream.

4.2.2 Redox Activity of Extra Clair Cream on Bare Carbon Graphite Electrode.

The carbon graphite working electrode was polished as already discussed elsewhere and the electrode modified using Extra Clair by attachment on the electrode surface. The modified electrode was subjected to electrolyte stability test whereby, the modified electrode was dipped into the various electrolyte solutions to be used in the analysis and assessed for stability on the electrode surface. The observations were that, there were no disintegrations or significant swelling of the cream and/or dissolution into the electrolyte. This stability was further confirmed from physical tests on the solubility of the Extra Clair cream in various solvents, aqueous and non-aqueous.

This electrode was then put in various solutions containing different concentrations H_2SO_4

(0.1M, 0.5M, and 1.0 M). The potential of the electrode was then cycled from -0.30V

0.90V at a scan rate of 20 mV/sec. The cyclic voltammetric response showed a very broad

Oxidation band and a relatively well defined reduction peaks at 0.36V, 0.39V and 0.44V in

0.1M, 0.5M and 1.0M H_2SO_4 respectively. See Figure 4.14

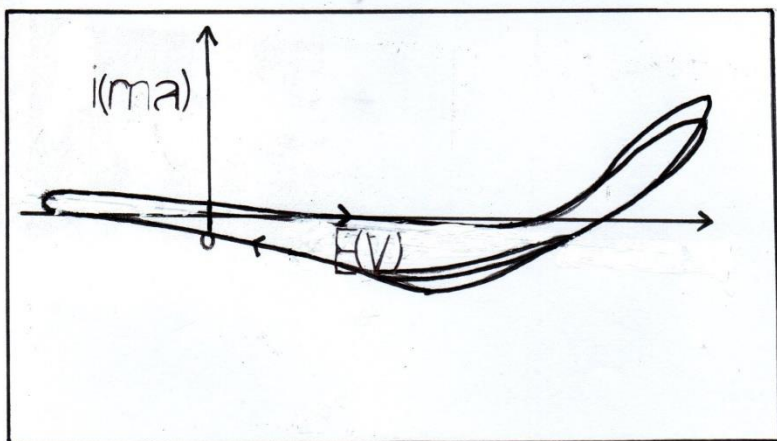


Figure 4.14: Cyclic voltammetric response for Extra Clair modified electrode in 0.1M, 0.5M and 1.0M H_2SO_4 . Potential range: -0.30V to 0.90V. Scan rate 20mV/s. **CV Scale:** 0.09V/cm (x-axis): 0.02mA/cm (y-axis)

This positive shift in reduction potential with increasing pH is an indication of the significance of protonation-deprotonation equilibria in the extra Clair redox process. The fact that, the broad Oxidation band is not affected by pH suggests this redox process is not reversible hence a strong pointer to non-equivalence of the redox centers i.e., the oxidation-reduction potentials for the various redox processes are not the same.

When the scan rate dependence studies were conducted on the Extra Clair modified electrode in 0.1M, 0.5M and 1.0M S H_2SO_4 (Figure 4.15).

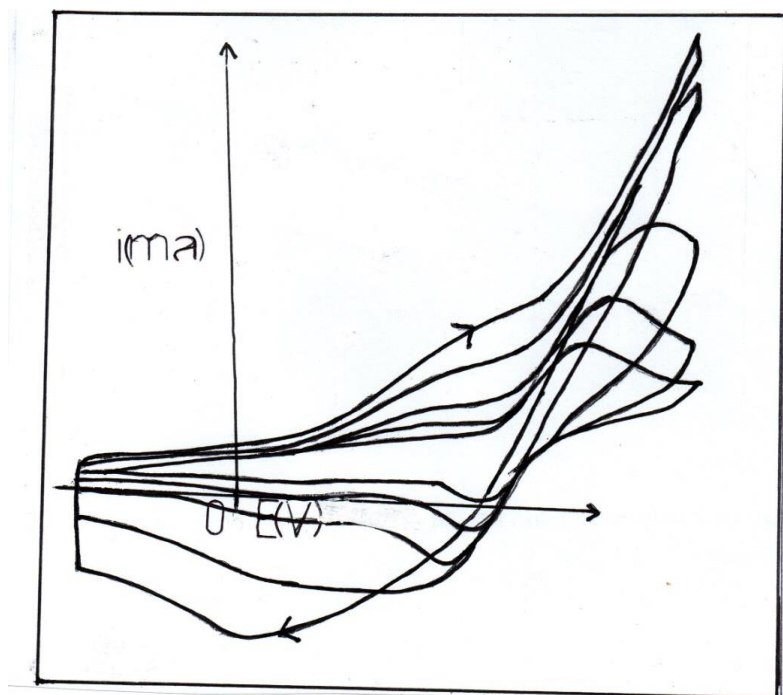


Figure 4.15: Variation of scan rate studies for Extra Clair modified electrode. Potential range: -0.30V to 0.90 V. Scan rates: 5mV/s, 10mV/s, 20mV/s, 50mV/s and 100mV/s. **CV Scale:** 0.09V/cm (x-axis): 0.02mA/cm (y-axis)

It is observed that the reduction peaks become increasingly well-defined at higher scan rates i.e. 100mv/sec. the oxidation peak remains broad and mishapened with peak tailing at low scan rates, a pointer to a diffusion limited process. This is confirmed by the linear plot obtained when the reduction peak current is plotted versus square of scan rate.

The Extra Claire modified electrode was subjected to potential window variation analysis i.e., the potential was varied from -0.30V (constant) to varying positive potential limits (0.70V, 0.75V, 0.80V, 0.85V, and 0.90V) there was no change in the redox peak profile with the oxidation peak currents remaining constant while the reductive peaks currents increased with the increasing positive potential limit. This observation once again a veiled pointer to the non-equivalence of the redox centers, or a ce type reaction (chemical-electrochemical). Such reactions would not be

surprising, given that from IR spectral analysis, several spectral bands associated with aromatic, saturated hydrocarbons and hydroxyl functional groups were observed to be present in Extra Clair cream.

The oxidation and reduction potentials did not vary with the positive potential limits.

4.2.3 Redox properties of Extra Clair cream on polyaniline modified electrode.

The carbon graphite working electrode was modified with polyaniline as already discussed in the thesis.

The polyaniline electrode was then modified with the Extra Clair cream and the electrode

This electrode then had its potential cycled from -0.30 V to varying positive potential limits (0.70V, 0.75V, 0.80V, 0.85V and 0.90V) in a 1.0 NaCl electrolyte solution. The resultant cyclic voltammogram (see Figure 4.16) yielded an inefficient quasi reversible redox process where the incremental increase in the oxidative peak current does not correspond to the increase in the reductive peak current.

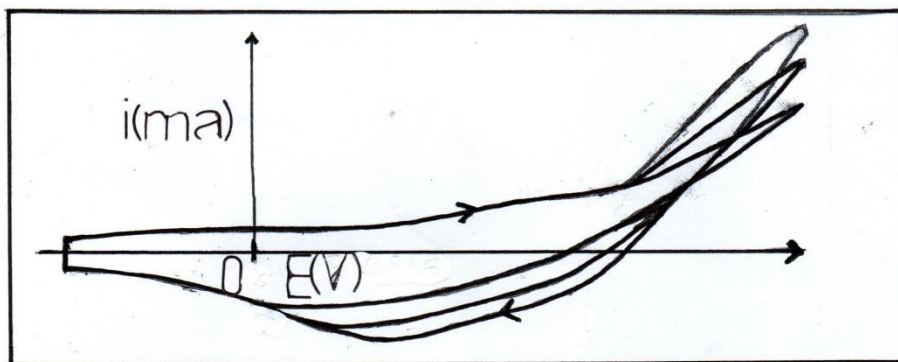


Figure 4.16: Cyclic voltammetric response for Extra Clair/PANI electrode in 1.0M NaCl. Potential range:-0.3V to 0.70V, 0.80V, 0.85V and 0.90V. Scan rate 20mV/s. **CV Scale:** 0.09V/cm (x-axis): 0.02mA/cm (y-axis)

The oxidative potentials occur at approximately 0.39V while the reductive peak potentials vary from 0.40V to 0.43V with the reductive peak current increasing as the positive potential limit is reduced. When the scan rate was varied for the case where the potential window was from -0.3V to 0.90V well defined oxidative and reduction peaks were observed at low scan rates (5mV/s, 10mV/S and 20mV/s) while at higher scan rates (50mV/s and 100mV/s), broad mishapened peaks which appear to have polyaniline redox characteristics appear. This non-detection of Extra Clair redox peaks at higher scan rates is more likely a pointer to the time dependence of the concentration of Extra Clair redox sites, rather than an inhibitory role of the PANI host matrix. When the Extra Clair- polyaniline modified electrode was transferred to a 0.1M NaCl electrolyte solution and the potential window varied from -0.30V to varying positive potential limits (0.70V, 0.75V, 0.80V, 0.85V and 0.90V) it is observed that poorly defined redox peaks are obtained as compared to the case of 1.0M NaCl electrolyte solution. This suggests that, the concentration of the supporting electrolyte affects the electron transfer kinetics in the Extra Clair redox process. On variation of scan rate, it is observed once again that the oxidative peaks are well defined at low scan rate as was the case in 1.0M NaCl (see Figure 4.17)

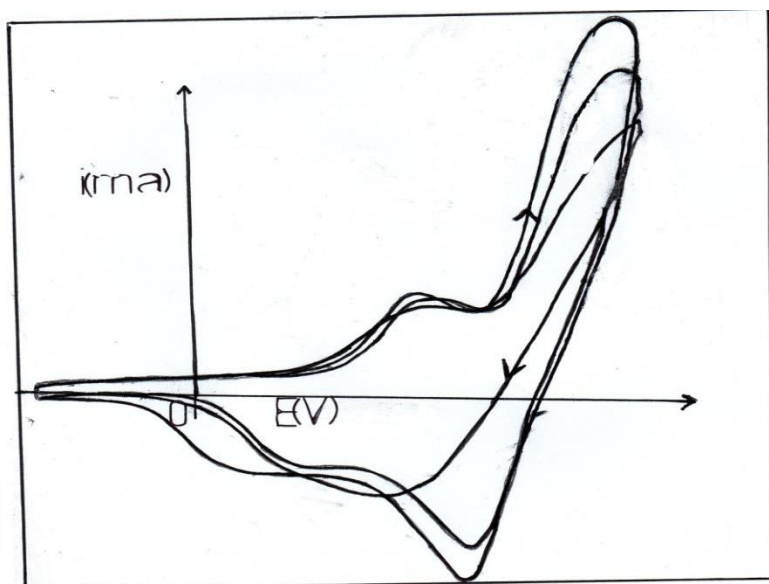


Figure 4.17: Scan rate dependence studies for Extra Clair-PANI modified electrode in 1.0M NaCl. Potential range: -0.3V to 0.70V,0.75V, 0.80V,0.85V and 0.90V. **CV Scale:** 0.09V/cm (x-axis): 0.02mA/cm (y-axis)

The glaring difference in the redox profile of the Extra Clair in 0.1M NaCl and 1.0M NaCl is captured in resultant cyclic voltammogram (see Figure 4.18). When the supporting electrolyte was changed to 1.0 M HCl, the redox process of Extra Clair on polyaniline electrode was significantly altered. The oxidative and reductive peaks of the Extra Clair redox process are now well defined. Polyaniline redox peaks appear recessive i.e., they appear as broad misshapened bands. Variation of potential window did not yield significant shifts in the Extra Clair oxidation reduction peaks.

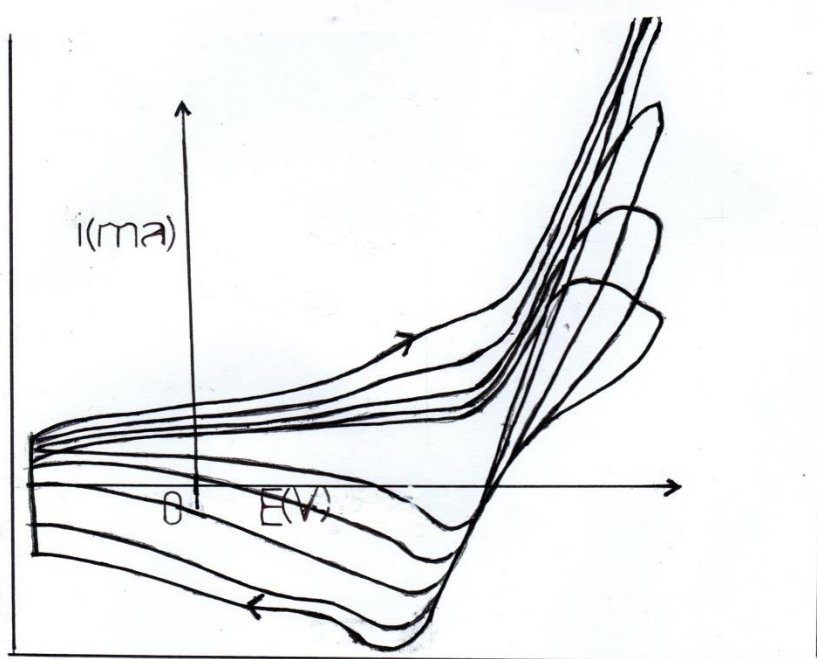


Figure 4.18: Differences in the redox profile of Extra Clair-PANI in 0.1M and 1.0M NaCl supporting electrolyte solution. Potential range: -0.30V to 0.90V. Scan rate 20mV/s. **CV Scale:** 0.09V/cm (x-axis): 0.02mA/cm (y-axis)

The well-defined peaks associated with the Extra Clair redox process can be attributed to the presence of hydrogen ions (protons). It is known that, the transfer of protons via the Grotthuss mechanism is much faster, hence improvement in the redox kinetics (P.W. Atkins 'Physical Chemistry', 6th Edition, Oxford Press). As was in the case of NaCl, it is observed that much more well defined oxidative and reductive peaks appear as in the case of Extra Clair redox process at lower scan rate.

The polyaniline redox peaks are once again broad, mishapened and recessive. It appears that the time dependence of the concentration of the Extra Clair redox center is not affected by the nature of the cation (Na^+ and H^+). When the concentration of HCl in the electrolyte is increased the oxidation and reduction peaks shift towards positive potentials. This is a pointer to the dependence of Extra Clair redox process on the protonation-deprotonation equilibria. The shift in

pH with potential is approximately 67mV/ pH, which suggest that, it is not strictly $1\text{H}^+/1\text{e}^-$ redox process. See Figure 4.19.

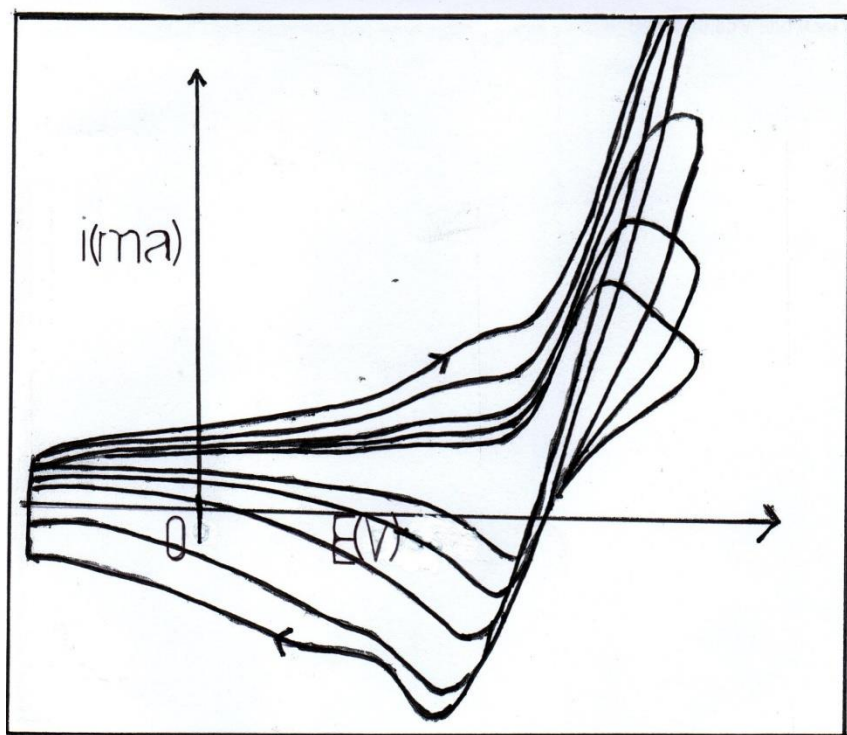


Figure 4.19: Effect of solution pH on Extra Clair –PANI electrode. Potential range: -0.30V to 0.90V. Scan rate 20mV/s. **CV Scale:** 0.09V/cm (x-axis): 0.02mA/cm (y-axis)

When the supporting electrolyte was changed to sulphuric acid, the same cyclic voltammetric response is obtained when the potential window is varied from -0.30V to varying positive potential limits (0.70V, 0.75V, 0.80V, 0.85V and 0.90V) in all the cases. The scan rate variation similarly showed well defined oxidation/ reduction peaks at low scan rate but poorly defined peaks at higher scan rates. This similarity in behavior when HCl was used as supporting electrolyte suggest that anion type (SO_4^{2-} and Cl^-) does not affect significantly the Extra Clair

redox process.

Further analysis of the Extra Clair redox process in supporting electrolyte containing 0.1 M, 0.5M and 1.0M H₂SO₄, reveal that, at positive potential limit corresponding to 0.70V and 0.75V no reduction and oxidation peaks were observed for Extra Clair. It is only above the 0.80V positive potential limit that the oxidation and reduction peaks appeared. This implies that the precursors in the Extra Clair redox process are formed at above 0.80V potential limit (Orata and Buttry,1987)

It is also observed when the Extra Clair -PANI modified electrode had its potential cycled from 0.30V to 0.90V at a scan rate of 20mV/s in H₂SO₄ supporting electrolytes of different concentrations (0.10M, 0.50M and 1.0M) It is observed that, the redox peaks are broad and misshapened. See Figure 4.19. This suggests slow electron transfer kinetics i.e., poor faradaic processes.

This is unlike in the case of bare carbon graphite electrode where, well defined quasi reversible redox peaks are obtained. This difference is probably attributable to the effect of the polyaniline host matrix. It is also [possible that, there is interference between the polyaniline and the Extra Clair redox centers leading to slow electron transfer i.e., increase in the Gibbs free energy. This is probably suggestive of a bilayer conformation rather than formation of a composite i.e., limited charge rectification.

4.2.4 Electro catalytic role of p-aminophenol in the Extra Clair redox process.

The Extra Clair –PANI modified carbon graphite electrode had its potential cycled from -0.3 V to varying positive [potential limits (0.70V, 0.75V, 0.80V, 0.85V and 0.90V) at a scan

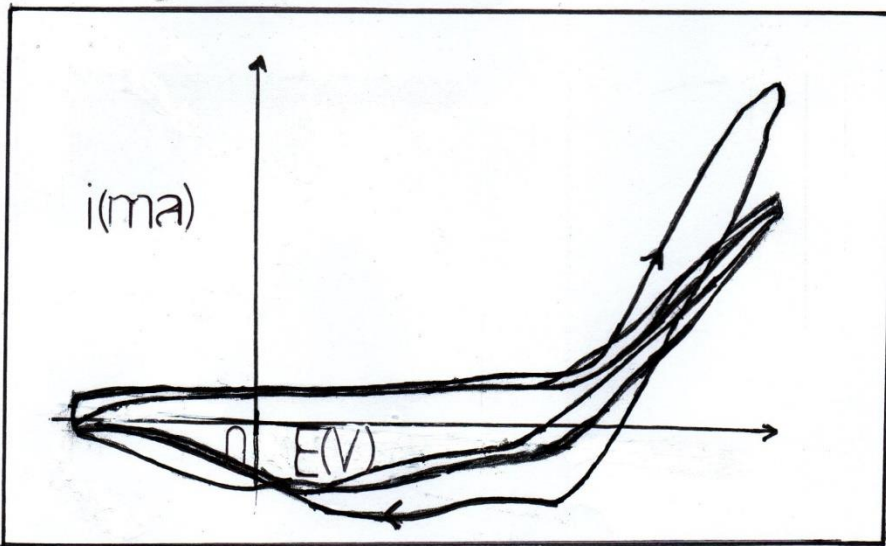


Figure 4.19: Effect of electrolyte solution (H_2SO_4) concentration on Extra Clair-PANI redox process. Potential range: -0.30V to 0.90V . Scan rate 20mV/s . **CV Scale:** 0.09V/cm (x-axis): 0.02mA/cm (y-axis)

rate of 20mV/s the electrolyte solution contained 1.0 M HCl and $0.01\text{M p-aminophenol}$. The resultant cyclic voltammetric response (see Figure 4.20) showed well defined redox peaks for the polyaniline redox process with the oxidation potential at 0.405 V and the reduction potential at 0.214V . The polyaniline redox potential remain relatively constant despite variation of the positive potential limit. It is important to mention that polyaniline oxidation and reduction potential on bare carbon graphite occurs at much lower potentials i.e., 0.19V and 0.03V respectively. This significant positive shift in the redox potentials can be attributed to multiple interaction between redox centers of Extra Clair, polyaniline and p-aminophenol. It is expected that the p-aminophenol removes the oxidative stress on polyaniline hence expected to lower the oxidation and reduction potential (Evans J.F et al., 1971)

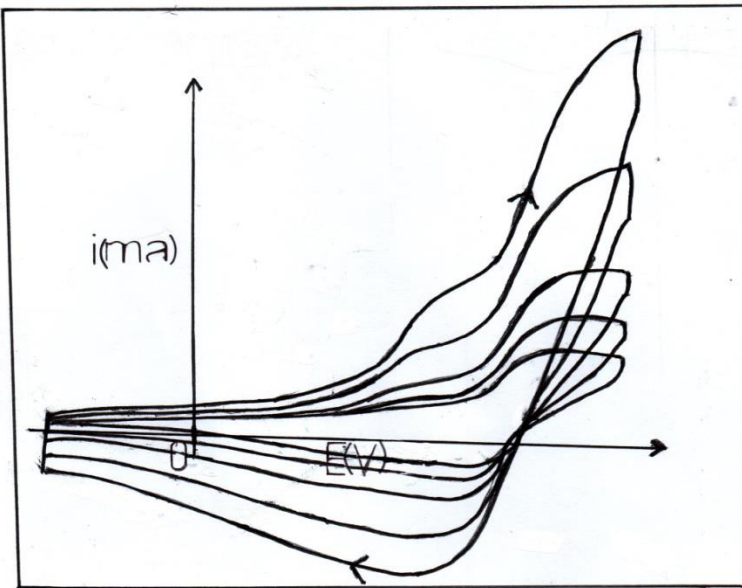


Figure 4.20: Extra-Clair –PANI redox process in 1.0 M HCl and 0.01M p-aminophenol. Potential range: -0.30V to 0.90V. Scan rate 20mV/s. **CV Scale:** 0.09V/cm (x-axis): 0.02mA/cm (y-axis)

Since this is not the case, this positive shift is dominantly the result of interaction between the Extra Clair and polyaniline redox centers. It is further observed that the Extra Clair oxidation/reduction peak occur at 0.73V/ 0.49V compared to the Extra Clair redox potential in the absence of p-aminophenol. It is observed that there is a significant decrease in the oxidation reduction for the Extra Clair redox process (81mV and 90mV for oxidation and reduction potential respectively) therefore in the case of the Extra Clair redox process, it appears that the p-aminophenol plays an electro catalytic role i.e., removes the oxidative stress in the Extra Clair redox process. Therefore this electrochemical dichotomy in the role of p-aminophenol can be attributed to entropic changes resulting from the interaction between redox centers with opposite net effect on the Gibbs free energy. In addition it is worth mentioning that other than the increased stress in polyaniline redox process, its electrochemical integrity has been preserved

i.e., well behaved redox process, easy electro-synthesis and reproducible electrochemical profile. The redox peaks attributed to Extra Clair is probably a composite peak consisting of the quinonic compounds resulting from the p-aminophenol redox process and the degradation of polyaniline at far positive potentials.

Potential window studies were conducted on Extra Clair-PANI modified electrode by cycling the potential from -0.30V to varying positive potential limits from 0.70V to 0.90V in increments of 50mV at a scan rate of 20 mV/s in 0.5M HCl electrolyte solution. No significant changes were observed in the resultant cyclic voltammetric response. The oxidation and reduction peak potentials remained unchanged. When the scan rate were varied, linear plots are obtained on plotting anodic peak current versus the square root of scan rate for the Extra Clair redox process. This suggests that the process is diffusion limited.

The polyaniline redox process yielded linear plots for peak current versus scan rate, an indication that the polyaniline is a surface attached species.

The effect of solution electrolyte pH was studied by cycling the potential of Extra Clair –PANI modified electrode in in electrolyte solution containing 0.1M, 0.5M and 1.0M hydrochloric acid. With the potential cycled from 0.3V to 0.90V at a scan rate of 20mV/s. It is important to mention that, the pH analysis was achieved by replacing the electrolyte solution in the electrolytic cell with solutions of varying HCl concentration. The same Extra Clair-PANI electrode was used throughout in the pH analysis. The resultant cyclic voltammetric response is shown in Figure 4.21.

As expected the polyaniline redox peaks shift positively as the pH of the electrolyte solution was lowered. On varying the electrolyte solution concentration from 0.1M to 0.5M HCl and 1.0M HCl, the positive shift in the reduction potential was 139mV and 129mV respectively.

It is observed that, there is slight inconsistency in the potential shift, in that the shift at 1.0M HCl is lower by 10mV as compared to that of 0.5M HCl. In all the cases, the pH effect is attributed to protonation-deprotonation equilibria in the redox process.

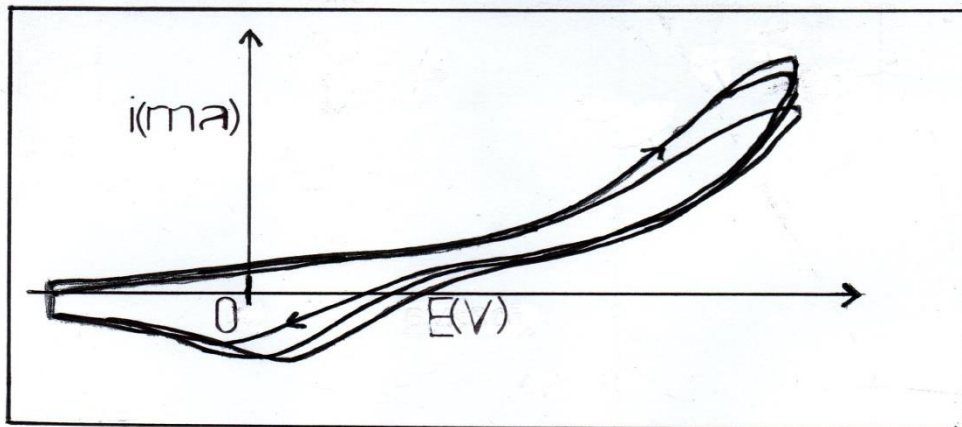


Figure 4.21: The effect of solution pH on the Extra-Clair –PANI electrode. Potential range: -0.30V to 0.90V. Scan rate 20mV/s. **CV Scale:** 0.09V/cm (x-axis): 0.02mA/cm (y-axis)

It is observed that the potential shift per pH unit is 129mV/pH. Hence, the redox process appears to be a $2\text{H}^+ / 1\text{e}^-$ process consistent with the Quinone redox process in polyaniline at far positive potentials. The ideal 120mV/pH shift is probably not observed because of the multiplicity of the redox processes responsible for the quinonic compounds. When the electrolyte solution was changed to sulphuric acid, it is observed that the cyclic voltammetric response is characterized by a very broad misshapened band. The polyaniline and the Extra Clair redox centers are not as distinct as was in the case of HCl as supporting electrolyte. This can be attributed to the $\text{SO}_4^{2-} / \text{HSO}_4^-$ anions. The mechanics of their effects or influence on the multiple redox centers can only be speculative, but it appears that the broad bands suggest a continuum in the redox potentials of

the various redox centers.

4.2.6. Redox activity of Extra Clair cream on bare carbon graphite working electrode in the presence of p-aminophenol

The bare carbon graphite working electrode surface was modified using Extra Clair cream as already discussed elsewhere in the thesis. The potential of this electrode was cycled from -0,3V to 0.90V at a scan rate of 20mV/s in an electrolyte solution containing 0.01M p-aminophenol and 1.0M HCl. A distinct reduction peak was observed at 0.56V and abroad shoulder observed at approximately 0.43V for the oxidation process. Interestingly as the potential increased there was a scaffolding as the oxidation peak current increased. This scaffolding is reminiscent of a nucleation process typical of redox process involving metal salts. This observation probably is a veiled pointer to the presence of metallic elements in the Extra Clair cream. This requires further research. It is noteworthy that, this redox profile appears to be repeated as the positive potential limit is increased (from 0.70V to 0.90V) The reduction peaks potentials shifted negatively with increasing positive potential limit. The negative shift with increasing potential limit as indicated earlier is probably the result of electro-catalytic role of p-aminophenol. When the scan rate was varied, the scaffolding of the oxidation peak was observed for 5mV/s, 20mV/s, 50mV/s and 100mV/s. But for the redox processes at 10mV/s, the scaffolding was not observed but instead a current spike typical of 1st scan response in electronically conducting polymers when they are switched from the insulating to the conducting state in low pH solutions was observed. A phenomenon associated with changes in the solvent population in the polymer (Orata and Buttry

1987, Orata et al 1997)

This current spike associated with redox peak at 10mV/s can therefore be attribute to changes in solvent population /and or formation of a redox junction. This assertion is strengthened by the observation that at high pH (0.1M Hall, 0.5M Hall) no scaffolding nor oxidation peak was observed (see Figure 4.22).

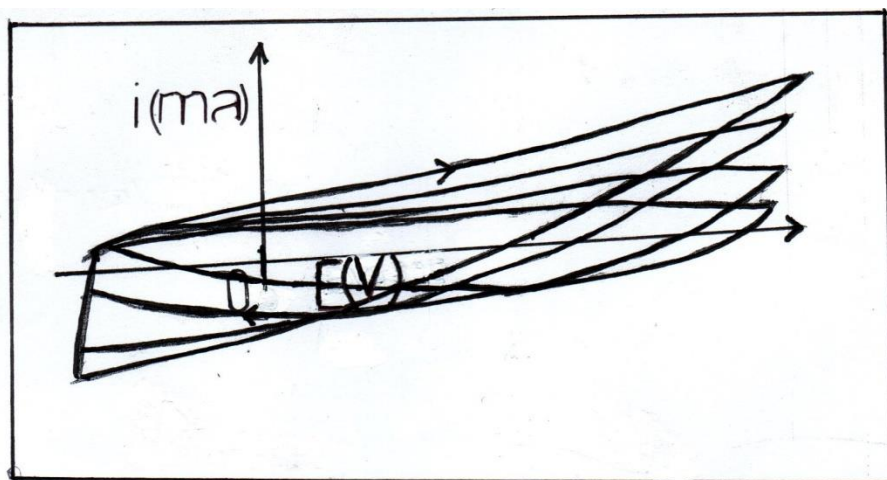


Figure 4.22: Redox activity of Extra Clair modified carbon graphite electrode in 1.0M HCl and 0.01M p-aminophenol. Potential cycled from -0.3V to 0.9V at scan rates of 5mV/sec, 10mV/sec, 20mV/sec, 50mV/sec and 100mV/sec. **CV Scale:** 0.09V/cm (x-axis): 0.02mA/cm (y-axis)

When the Extra Clair modified carbon graphite working electrode had its potential cycled in an electrolyte solution containing 1.0 M H₂SO₄ (see Figure 4.23). The potential was cycled from -0.3V to 0.9V at varying scan rates of 5mV/sec, 10mV/sec, 20mV/sec, 50mV/sec and 100mV/sec. No scaffolding or current spike was observed for the oxidation peak. A broad

oxidation shoulder was observed in the range 0.41V- 0.50V, as the scan rate is varied from 5mV/s to 100mV/s. A well -defined oxidation peak is observed at 0.71V and 0.78V at scan rates of 5mV/s and 10mV/s respectively. The reduction peaks shift towards negative potentials with increasing scan rate in the range of 0.75V - 0.43V. This negative shift in the reduction peak potential was similarly observed in HCl electrolyte media. The absence of the scaffolding /current spike previously observed in the oxidation process associated with Extra Clair can be attributed to a suppression of nucleation processes by $\text{SO}_4^{2-}/\text{HSO}_4^-$ anions. No significant change in the redox profile was observed on variation of the positive potential limit from -0.30V constant, to 0.70V, 0.75V, 0.80V, 0.85V and 0.90V.

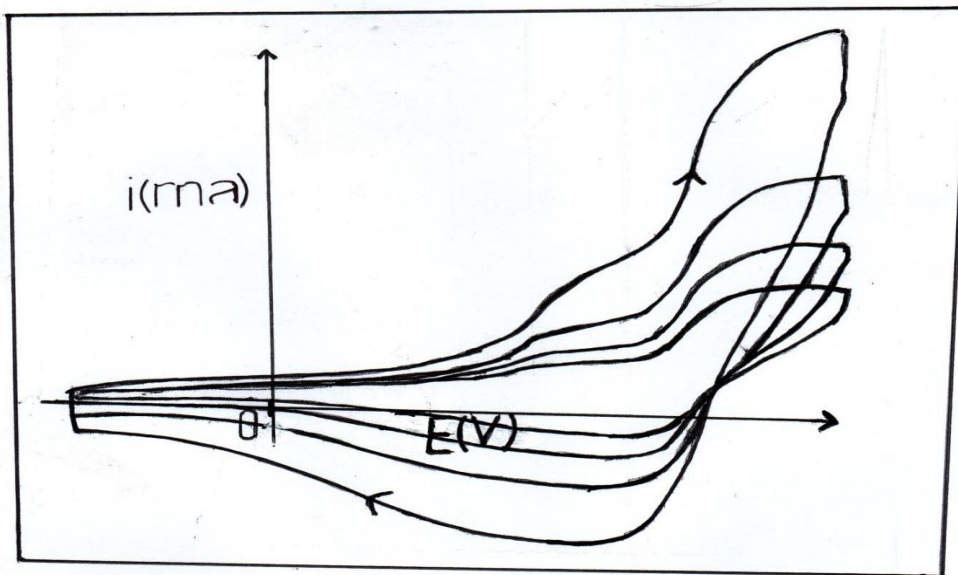


Figure 4.23: Redox activity of Extra Clair modified carbon graphite electrode in 1.0M H_2SO_4 and 0.01M p-aminophenol. Potential range: -0.30V to 0.90V . Scan rate 20mV/s . **CV Scale:** 0.09V/cm (x-axis): 0.02mA/cm (y-axis)

When the pH of the electrolyte solution was varied (0.1M and 0.5 M Sulphuric acid) , it is observed that at 50mV/s and 100mV/s two reduction peaks are observed at 0.17V and 0.12 V and a second peak at 0.41 V for 50mV/s / 100mV/s respectively. See Figure 4.24 . It is proposed that the $\text{SO}_4^{2-}/\text{HSO}_4^-$ anions are responsible for the formation of the two redox centers probably as a result of a chemical reaction. That these centers are observed at high scan rates suggest the transient/ intermediary nature of the chemical process.

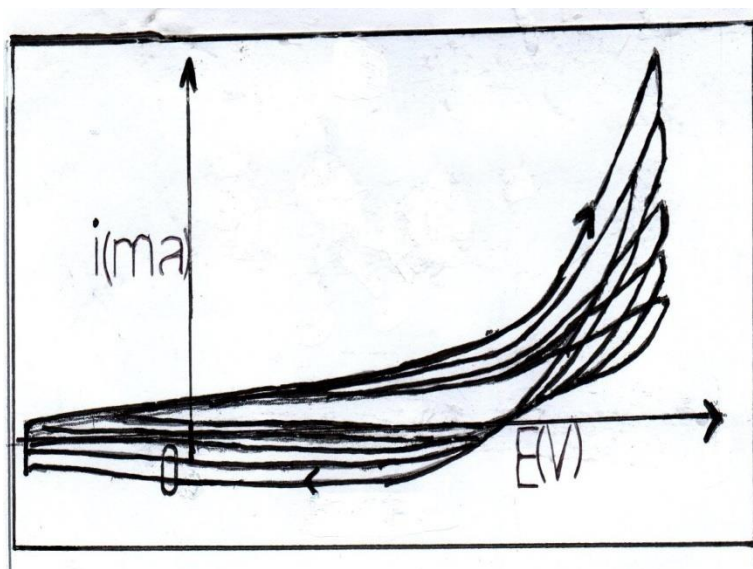


Figure 4.24: Effect of solution pH on the redox activity of Extra Clair modified carbon graphite electrode in 0.1M and 0.5M H_2SO_4 . Potential range: -0.30V to 0.90V. Scan rate 20mV/s. **CV Scale:** 0.09V/cm (x-axis): 0.02mA/cm (y-axis)

That the chemical process proposed above as responsible for transient/intermediary product is strongly pH dependent is captured in the observation that the double reduction peaks are observed now at low scan rates (20mV/s) in 1.0M H_2SO_4 .

4.2.7 Redox activity of Extra Clair on Bentonite modified electrode

A carbon graphite working electrode was modified with bentonite as already discussed elsewhere in the thesis. This electrode was further modified with Extra Clair. The potential of this electrode was cycled from -0.30V to 0.90V at a scan rate of 20mV/s in an electrolyte solution containing 1.0M H₂SO₄. The cyclic voltammetric response is characterized by a poorly defined oxidation peak and well-defined reduction peaks at 0.84V and 0.48V respectively. These peaks are attributed to the

Extra Clair redox process for there are no known redox peaks associated with bentonite and carbon graphite (see Figure 4.25).

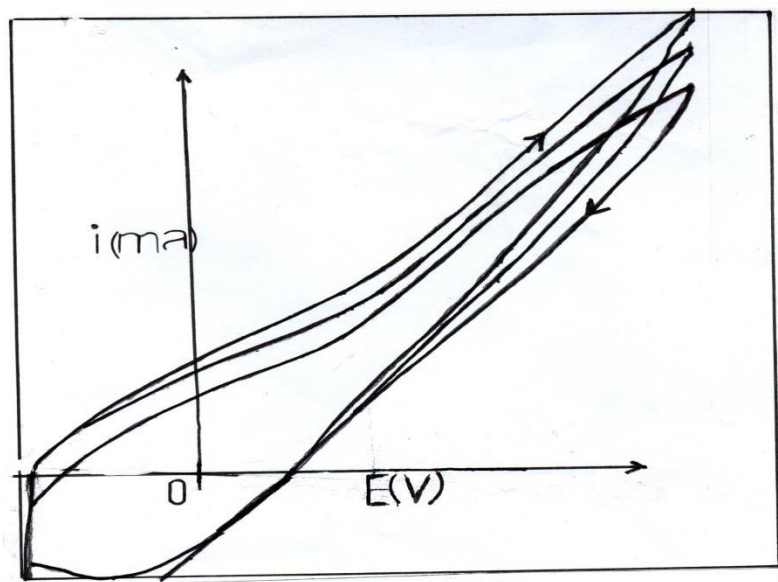


Figure 4.25: Redox activity of Extra Clair-Bentonite electrode in 1.0M H₂SO₄. Potential range: -0.30V to 0.90V. Scan rate 20mV/s. **CV Scale:** 0.09V/cm (x-axis): 0.02mA/cm (y-axis)

Variation of the positive potential limit from -0.30V to 0.70V, 0.75V, 0.80V, 0.85V and 0.90V did not affect the oxidation and reduction potential significantly. When the scan rates were varied, the reduction peak potentials shifted significantly negatively by 162mV for the range 5mV/s to 100mV/s. The oxidation peak potential remained relatively constant. On computation it is observed that the peak current (oxidative/reductive) does not vary linearly with the square root of scan rate suggesting that the process is not diffusion limited. Variation of potential window from - 0.30V to various positive limits (0.70V to 0.90V in increments of 50mV) yielded broad reduction peaks with potentials at 0.48V, 0.45 V, 0.43V for the positive potential limits, 0.80V, 0.85V and 0.90V respectively.

At 0.70V and 0.75V positive potential limits, the reduction peak was broad and misshapened but with two poorly defined peaks at 0.21 V. It is noteworthy that, the reduction peak potential shifted negatively for cases where the potential limit was above 0.80V. This lowering of the reduction potential can be attributed to the bentonite host matrix, since in the case of bare carbon graphite electrode there were no shifts in the reduction potential. Bentonite is known to have a non-pillared structure consisting of tetrahedral (T_d) and octahedral (O_h) sites, with the latter occupied by metal cations. Thus its influence can result from a combination of structural stabilization and electronic interaction of metal cations with the Extra Clair redox centers.

4.2.8 Extra Clair cream –Bentonite composite on carbon graphite working electrode.

Extra Clair cream-bentonite composite was prepared by mixing equal amounts of Extra Clair cream and bentonite (w/w), the two were mixed to form a fine uniform paste. The carbon

graphite working electrode was then modified using the paste/composite. This electrode had its potential cycled from -0.30V to 0.90V at varying scan rates in electrolyte solutions containing 0.1 M, 0.5M and 1.0M H₂SO₄ (see Figure 4.26)

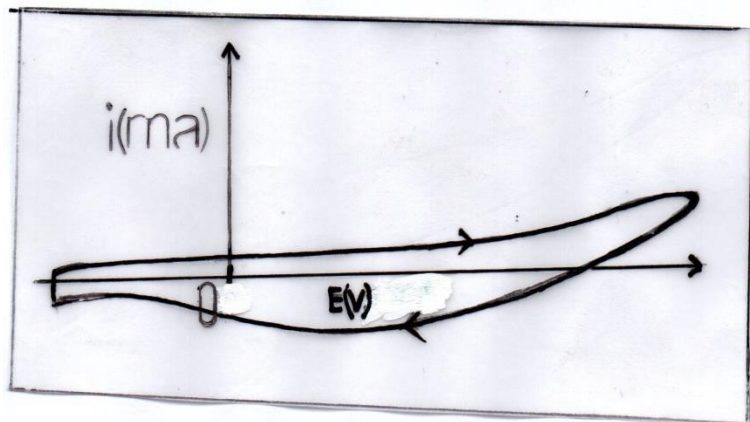


Figure 4.26: Cyclic voltammetric response of Extra Clair/Bentonite composite Modified electrode in 0.1M, 0.5M and 1.0M H₂SO₄ solutions. Potential range: -0.30V to 0.90V. Scan rate 20mV/s. **CV Scale:** 0.09V/cm (x-axis): 0.02mA/cm (y-axis)

The resultant cyclic voltammetric response shows broad oxidation peaks at approximately 0.76V for all the scan rates. The reduction peak potential on the other hand shows significant shifts towards lower potentials as the scan rate increases (0.59V/5mV/s, 0.59V/10mV/s, 0.57V/20mV/s, 0.50V/50mV/s and 0.48V/100mV/s) It is proposed that, this shifts in the reduction peak potentials could be an indicator of time dependent structural/entropic changes in the Extra Clair redox centres.

It is also important to mention that, the electrolyte solution pH affect the redox process. It is observed that, as the pH is increased there is no definite reduction peak. This suggests that, the

structure of the redox centers associated with the reduction process is also not pH dependent.

Variation of the potential windows i.e., from -0.30V (constant) to 0.70V, 0.75V, 0.80V, 0.85V and 0.90V did not significantly change the redox profile of the Extra Clair cream –bentonite composite.

When the nature of the supporting electrolyte was changed from sulphuric acid to hydrochloric acid, and the potential cycled from -0.30V to 0.90V at a scan rate of 20mV/s, the resultant cyclic voltammetric response had no definite oxidation peak but had a well-defined reduction peak i.e. the redox process was irreversible. It was observed that, when the concentration of HCl is varied (0.1M, 0.5M and 1.0M) the reduction peak potentials shifted towards positive potentials i.e. 0.30V/ 0.1M HCl; 0.02V /0.5M HCl, and 0.08V/1.0M HCl. See Figure 4.27. This represents a very significant shift in the reduction potential for the case of HCl media, as compared to that observed in the case of sulphuric acid electrolyte media i.e., 547mV. This is a major difference, it strongly suggest non-equivalence of the redox centers. An observation which can be attributed to the difference in anion type i.e., Cl^- and $\text{SO}_4^{2-}/\text{HSO}_4^-$.

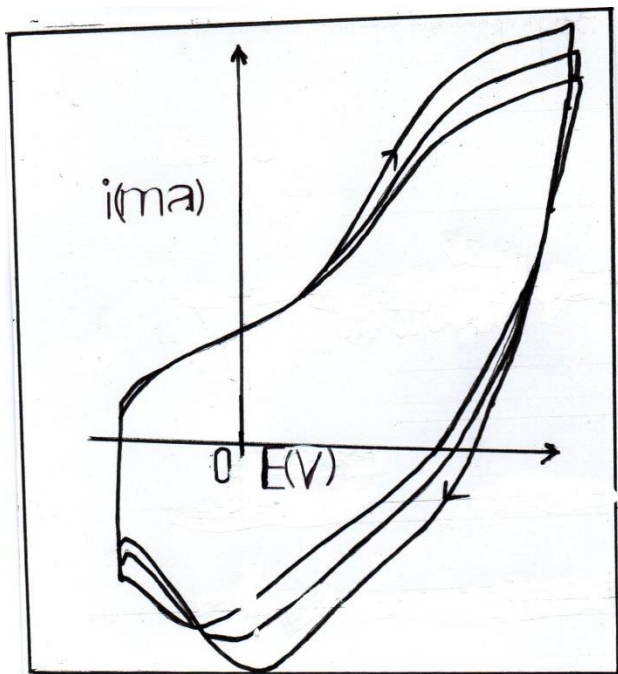


Figure 4.27: Effect of anion type on the Extra Clair/Bentonite composite redox process. Potential range: -0.30V to 0.90V. Scan rate 20mV/s. **CV Scale:** 0.09V/cm (x-axis): 0.02mA/cm (y-axis)

The mechanics of the interaction with the Extra Clair redox centers leading to these differences probably lies in the fact that, the chloride ion is small and has a high charge density, therefore can easily penetrate the bentonite matrix/ and or interact with the redox active centers in Extra Clair. The specific nature of interaction is therefore speculative.

4.2.9. Redox activity of Extra Clair cream on Polyaniline –Bentonite modified electrode

The bare carbon graphite working electrode was first modified using bentonite. Polyaniline was then electrodeposited on this electrode by cycling its potential from -0.20V to 0.85V at a scan rate of 20mV/s in an electrolyte solution containing 0.1 M aniline and 1.0M Sulphuric acid. This

electrode was then modified using Extra Clair cream, and had its potential cycled from -0.30V to 0.90V at varying scan rates in 1.0M H₂SO₄ electrolyte solution.

It is observed that a broad oxidation peaks appears at approximately 0.44V at all scan rates. The reduction peaks appear at 0.49V at 5mV/s, 0.46V at 10mV/s, 0.43V at 20mV/s, 0.40V at 50mV/s and 0.40 V at 100mV/s . It is once again observed that, the redox peaks potentials vary with scan rates suggesting time dependent structural variation of redox centers associated with the reduction process, as was the case in the absence of polyaniline. When the potential window variation studies were conducted by cycling the potential from -0.30V to 0.70V, 0.75V, 0.80V, 0.85V, and 0.90V at scan rate of 20mV/s, it is observed that, while the oxidation peak is completely suppressed, the reduction peak potential become increasingly well defined as the potential limit increases, in addition to shifting towards lower potentials. Varying the positive potential limits from 0.75V to 0.90V resulted in a 68mV shift in potential. It is important to note that, as the positive potential limit is increased, the Extra Clair redox process becomes irreversible. This probably suggests an **e-c** mechanism.

When the electrode potential was cycled from -0.30V to 0.90V at a scan rate of 20mV/s in an electrolyte solution of varying pH (0.1 M, 0.5M and 1.0M H₂SO₄). Once again, the process is irreversible i.e., no oxidation peak but well defined reduction peaks with the lowering of the solution pH. The improvement in the faradaic processes associated with the reduction once again can be attributed to the effect of protonation-deprotonation equilibria.

4.2.10 Effect of p-aminophenol on the redox properties of Extra Clair cream-Bentonite composite modified electrode

Extra Clair cream –bentonite composite used in modifying the carbon graphite working electrode was prepared as already discussed elsewhere in the thesis. The potential of this electrode was cycled from -0.30V to 0.90V at varying scan rates (5mV/s, 20mV/s and 50mV/s) in a solution containing 0.01M p-aminophenol and 1.0M H₂SO₄.

The resultant cyclic voltammetric response yielded two broad oxidation peaks occurring at approximately 0.45V and 0.78 V. The reduction peak potential occurred at approximately 0.55V. It is observed that there is a shift in the oxidation peak potential for the first oxidation peak as the scan rate is increased. When the scan rate is increased ten-fold i.e., from 5mV/s to 50mV/s, the positive shift in the oxidation potential is approximately 50mV. The second oxidation peak is unaffected by variation of scan rate. The reduction peak potential on the other hand shifts towards negative potential as the scan rate is increased. See Figure 4.29.

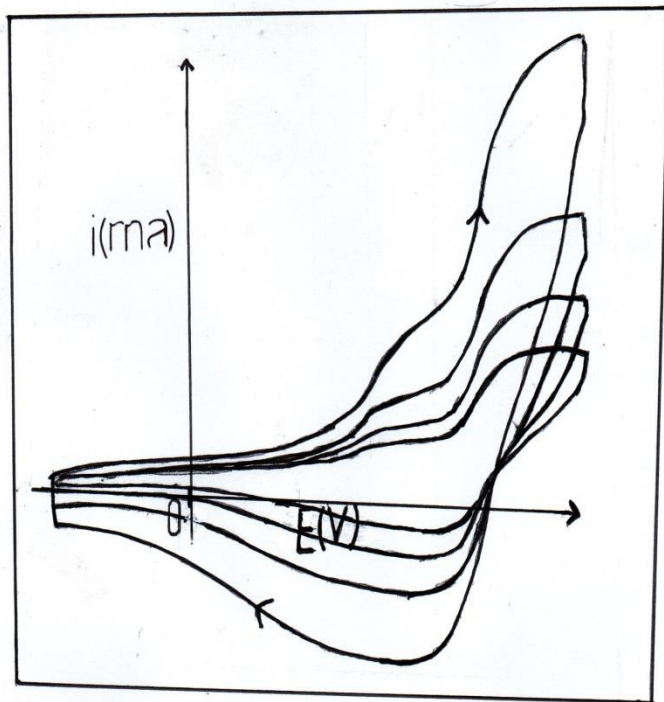


Figure 4.29: Effect of p-aminophenol on the Extra Clair-Bentonite composite redox process. Potential range: -0.30V to 0.90V . Scan rate 20mV/s . **CV Scale:** 0.09V/cm (x-axis): 0.02mA/cm (y-axis)

The observation that the first oxidation peak potential and the reduction peak potential vary with scan rate suggests time dependent structural / and or entropic changes associated with the redox centers. It is proposed that the Extra Clair redox active functionality (ies) interact with the bentonite matrix. The interaction could involve the isomorphously substitutable metal cations in the octahedral layer of the bentonite matrix. The second oxidation peak potential observed at 0.78V incidentally correspond to the Extra Clair-bentonite composite peak observed in the absence of 0.01M p-aminophenol. This therefore suggest a possible interaction between the extra Clair-bentonite redox center and the p-aminophenol redox active moiety. This suggestion is strengthened by the fact that, there is a negative shift of approximately 330mV . This negative

shift is probably the result of the electro-catalytic role of p-aminophenol in the total redox system i.e., removal of oxidative stress. It is also proposed that the reduction peak potential at 0.55V represents the Extra Clair-bentonite redox activity in the absence of p-aminophenol. When the positive potential limit was varied for the Extra Clair –bentonite modified electrode in 0.01M p-aminophenol and 1.0M sulphuric acid from 0.70V to 0.90V in increments of 50mV no significant change was observed in the cyclic voltammetric profile.

Further studies were conducted to establish the effect of anion type on the redox activity of Extra Clair –bentonite modified electrode. This involved use of 1.0M HCl as the supporting. The resultant cyclic voltammogram had no defined oxidation or reduction peaks. See Figure 4.30.

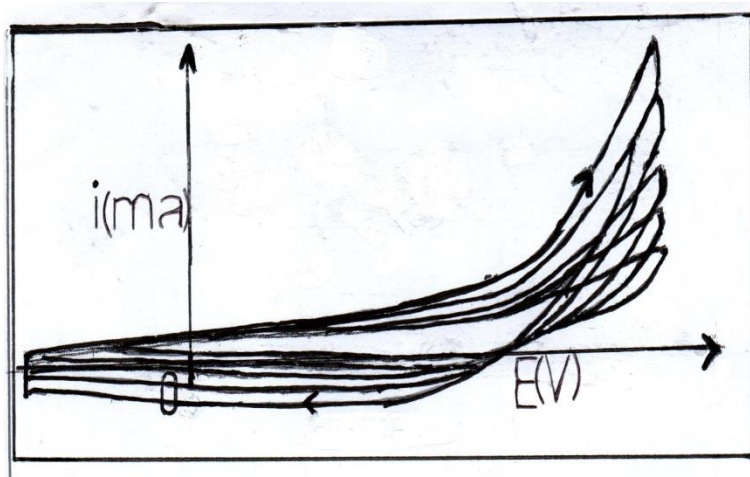


Figure 4.30 Cyclic voltammetric response of the Extra Clair-Bentonite composite in 1.0M HCl. Potential range: -0.30V to 0.90V. Scan rate 20mV/s. **CV Scale:** 0.09V/cm (x-axis): 0.02mA/cm (y-axis)

This apparent difference can be attributed to the effect of chloride ions. It is proposed that the chloride ion, having a high charge density because of its ionic radii can interfere significantly

with the electrodynamics between the Extra Clair redox moiety and the bentonite matrix. When the experiment was repeated in 1.0M NaCl supporting electrolyte, the resultant cyclic voltammogram was characterized by a broad poorly defined oxidation peak and a relatively well defined reduction peak at approximately 0.04V at 20mV/s scan rate. This improvement can be attributed to the change in cation type from H⁺ to Na⁺. It is proposed that this improvement in the faradaic process is the result of interaction of the Na⁺ with the bentonite matrix given that, it is isomorphously substitutable with the metal ions in the bentonite octahedral layer. It is important to note that, contrary to what is expected that, H⁺ whose movement is typified by the Grotthus mechanism did not lead to significant improvement in the faradaic process. This gives

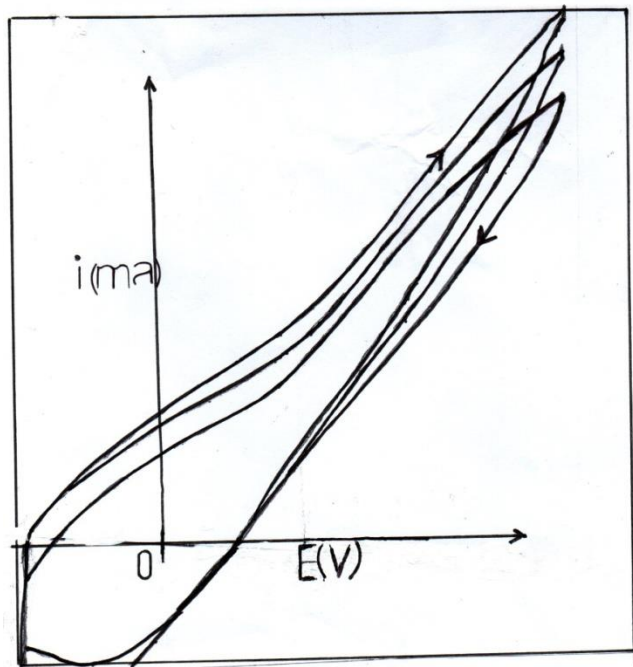


Figure 4.31: Cyclic voltammetric response of Extra Clair-bentonite electrode in 10% acetonitrile: 90% water with TBAP as supporting electrolyte. Potential range: -0.30V to 0.90V. Scan rate 20mV/s. **CV Scale:** 0.09V/cm (x-axis): 0.02mA/cm (y-axis)

credence to the Na^+ interaction with metal cation in the bentonite octahedral layer.

That the Na^+ is isomorphously substituted in the bentonite octahedral layer, hence affecting the nature of the bentonite host matrix interaction with the Extra Clair redox sites was further confirmed when the process was repeated in non-aqueous media containing (10% acetonitrile: 90% water and 0.01 M Tetrabutyl Ammonium perchlorate(TBAP).The resultant cyclic voltammetric response (see Figure 4.31) had no defined oxidation reduction peaks i.e.,poor faradic process. This poor redox response can be attributed to the bulky tetrabutyl ammonium cation which has a sizeable ionic radii and a low charge density therefore, cannot be isomorphously substituted in the bentonite octahedral layer. This confirms our earlier assertion

that, improvement observed earlier with NaCl supporting electrolyte was due to isomorphous substitution of sodium cations in the octahedral layer of the bentonite matrix.

4.3 ELECTROCHEMICAL ANALYSIS OF HYDROCORTISONE-MEDICATED CREAM

4.3.1. Redox activity of Hydrocortisone on bare carbon graphite working electrode

The bare carbon graphite electrode was modified using hydrocortisone cream by modified dip coating method. The modified electrode displayed the redox properties of the hydrocortisone when the potential was cycled from -0.30V to 0.85V at a scan rate of 20mV/s in various supporting electrolytes containing 0.1M , 0.5M and 1.0M H₂SO₄. The resultant cyclic voltammogram is shown in Figure 4.32.

The cyclic voltammetric response is characterized by reduction peaks occurring at 0.50V for the 0.1M sulphuric acid solution and 0.61V for the 0.5M and 1.0M Sulphuric acid solution. The reduction peaks are broad and misshapened. . There are no oxidation peaks. This redox process is not reversible and is possibly representing a **c-e-c** mechanistic pathway, where there is a chemical reaction involving the modification matrix followed by an electrochemical reaction on reversing the potential from 0.85V to 0.30V. On variation of scan rate from 5mV/s to 10mV/s, a significant negative shift in the reduction potential is observed as the scan rate is increased.

It is also important to mention that a broad and misshapened oxidation peak is observed at 5mV/s. This is a pointer to slow electron transfer kinetics /and or existence of multiple redox centers with a continuum in potentials.

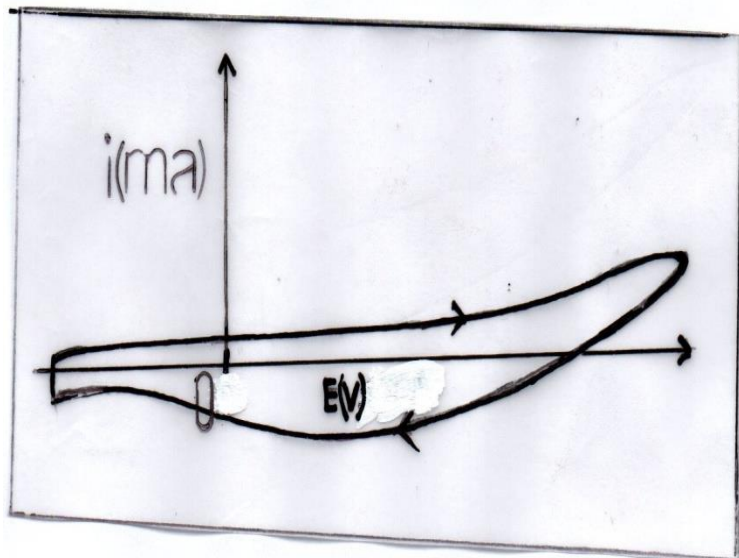


Figure 4.32: Cyclic voltammetric response of Hydrocortisone modified electrode in 0.1 M, 0.5M and 1.0M H_2SO_4 . Potential range: -0.30V to 0.90V. Scan rate 20mV/s. **CV Scale:** 0.09V/cm (x-axis): 0.02mA/cm (y-axis)

It was further observed that, on varying the potential limit in increments of 50mV from 0.70V to 0.90V the reduction peak potential shifts negatively with increasing potential limit, except for the 0.90V case where there was a slight positive shift in reduction potential. This negative shift in potential can be attributed to decrease in the Gibbs free energy/and or increase in entropy in the electrochemical system. The extent of the influence of this thermodynamic state functions depend on the state of the electrochemical redox center.

The hydrocortisone redox process is not very efficient as the incremental increase in the cathodic peak is not mirrored in the oxidation domain.

4.3.2. Hydrocortisone redox process in sodium chloride supporting electrolyte solution

The Hydrocortisone modified electrode had its potential cycled from -0.30V to 0.85V at 20mV/s in 0.1M, 0.5M and 1.0 M sodium chloride solutions. The resultant cyclic voltammograms are shown in Figure 4.33. A broad and misshapened reduction peak is observed. The absence of an

oxidation peak indicates that the redox process is irreversible. This poor electron transfer kinetics/poor faradaic processes displayed can be attributed to the absence of the protons (H^+), suggesting that, the hydrocortisone redox process is strongly dependent on protonation/deprotonation equilibria.

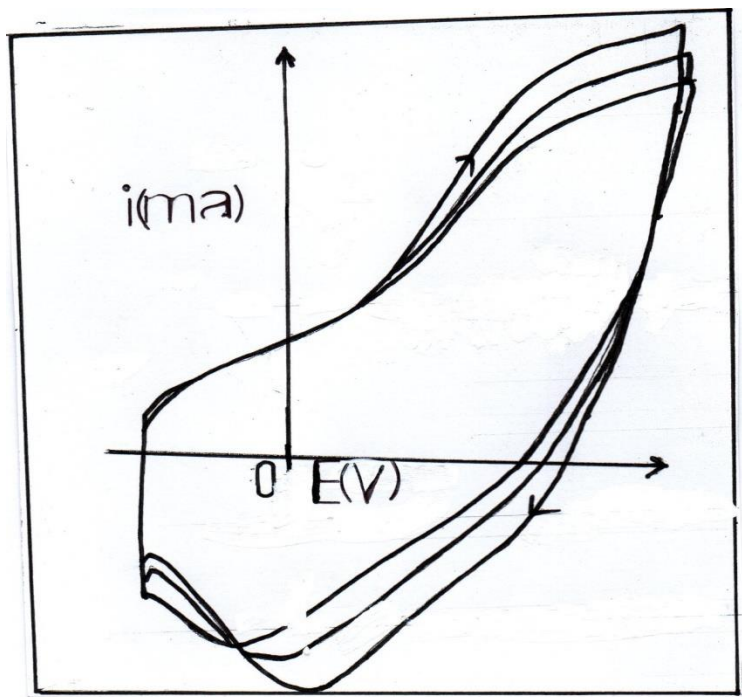


Figure 4.33: Cyclic voltammetric response of Hydrocortisone modified electrode in 0.1 M, 0.5M and 1.0M NaCl. Potential range: -0.30V to 0.90V. Scan rate 20mV/s. **CV Scale:** 0.09V/cm (x-axis): 0.02mA/cm (y-axis)

This assertion was confirmed when the hydrocortisone modified electrode was transferred to an electrolyte solution containing 1.0M Hydrochloric acid. The oxidation and reduction peaks occur at 0.70V and 0.53V respectively. The presence of the oxidation peaks which was not observable in the H_2SO_4 electrolyte media can be attributed to the presence of the chloride ion (Cl^-).

This suggests a change in the electrochemical mechanistic pathway from c-e-c to e-c-e or c-e.

The precise nature of the electrochemical intervention by the chloride anion leading to a change in the mechanistic pathway from **c-e-c** to **e-c-e** or **c-e** can be attributed to/ and or related to the fact that chloride ion has a small ionic radii and high charge density therefore is highly versatile. The precise interaction is purely speculative.

4.3.3.Redox behavior of Hydrocortisone on Polyaniline modified carbon graphite electrode.

The polyaniline modified electrode was obtained by cycling the potential of the carbon graphite working electrode from -0.20V to 0.85V in a solution containing 0.1M aniline and 1.0M sulphuric acid at a scan rate of 20mV/s.

The polyaniline (PANI) modified electrode was then modified with hydrocortisone. The of the hydrocortisone-polyaniline electrode was cycled from -0.30V to

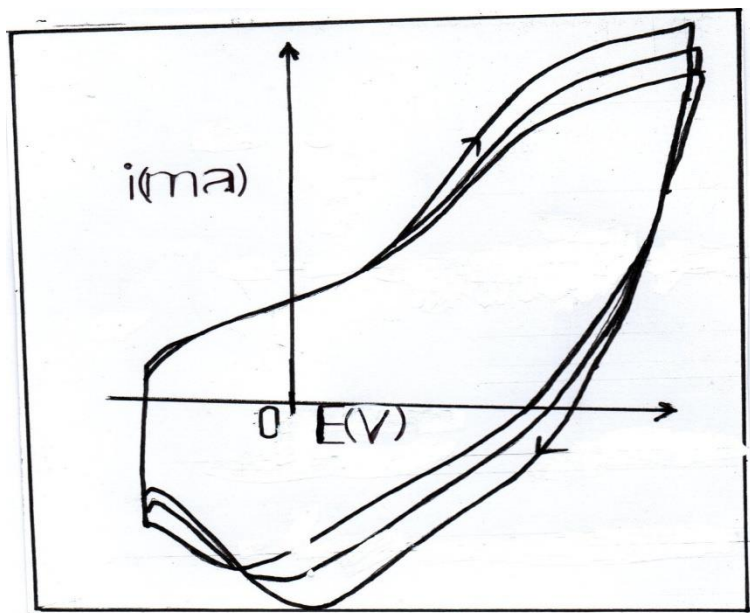


Figure 4.34: Cyclic voltammetric response of Hydrocortisone-PANI modified electrode in 0.1 M, 0.5M and 1.0M H₂SO₄. Potential range: -0.30V to 0.90V. Scan rate 20mV/s. **CV Scale:** 0.09V/cm (x-axis): 0.02mA/cm (y-axis)

0.85V at a scan rate of 10mV/s in electrolyte solutions containing 0.1M, 0.5M and 1.0M H₂SO₄ the resultant cyclic voltammetric response is shown in Figure 4.34.

Broad oxidation peaks and well defined reduction peaks are observed. The oxidation peak potential is observed at approximately 0.56V while the reduction peak potentials occur at 0.11V, -0.03V and 0.04V in the 0.1M, 0.5M and 1.0M H₂SO₄ electrolyte solutions respectively. From the voltammetric response it is apparent that the hydrocortisone-polyaniline no longer displays the redox properties of polyaniline. During the change in the electrolyte solution pH the oxidation peaks potential is invariant, while the reduction peak potentials shift positively. This is a further confirmation that the electrode no longer displays exclusively the electrochemical properties of polyaniline, which is known to be strongly pH dependent. It is apparent that the polyaniline host matrix affects significantly the redox behavior of hydrocortisone. This is based on the observation that, the reduction peak potential of hydrocortisone on bare carbon graphite electrode is significantly different from that obtained on the polyaniline modified electrode. In all the cases it is observed that the reduction peak potential of hydrocortisone in 0.1M, 0.5M and 1.0M H₂SO₄ is shifted negatively by 320mV, 330mV and 340mV respectively. Another marked difference is the observation that in the case of bare carbon graphite electrode there were no oxidation peaks. This is a veiled pointer to the fact that the polyaniline host matrix electrocatalyses hydrocortisone redox process. This is not surprising given that polyaniline redox pathway is characterized by an elaborate protonation/deprotonation equilibria. This assertion is further supported by the observation involving the

NaCl supporting electrolyte. On varying the scan rates, better redox profiles are obtained at lower scan rates (2mV/s and 5mV/s). This points to the time dependent transitory behavior of the oxidisable species. In addition at lower scan rates two reduction peaks are observed at 0.02V and 0.43V. This multiple reduction peak further confirms the significant influence of the polyaniline host matrix on the hydrocortisone redox process. The second reduction peak is probably the result of electrochemical interaction with the Quinone/imine derivatives which characterizes the redox behavior of polyaniline in the absence of aniline monomer in the electrolyte solution at far positive potentials.

Variation of the positive potential limit did not change significantly the hydrocortisone redox peak potentials (see Figure 4.35)

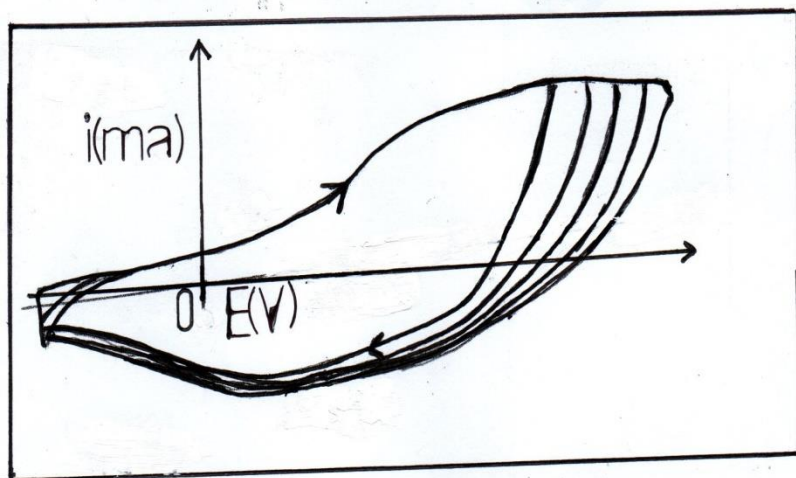


Figure 4.35: Effect of variation of positive potential limit on the Hydrocortisone-PANI modified electrode. Potential range: -0.30V to 0.90V. Scan rate 20mV/s. **CV Scale:** 0.09V/cm (x-axis): 0.02mA/cm (y-axis)

The hydrocortisone-PANI electrode was transferred to electrolyte solutions containing 0.1M,

0.5M and 1.0M hydrochloric acid and cycling the potential from -0.30V to 0.85V at a scan rate of 5mV/s. The resultant cyclic voltammetric response is shown in Figure 4.40. It is observed that there is significant degradation in the redox profile of the hydrocortisone. The redox peaks are broad and misshapened. It is important to mention that, an electrochemical 'node' is observed at -0.03V . This is probably reflective of isopotential phenomenon, resulting from equivalent redox centers in the hydrocortisone. This is probably once again resulting from interactions involving the highly versatile chloride ions. When the electrode was transferred to an electrolyte solution containing 0.1m, 0.5m and 1.0M sodium chloride and the potential cycled from -0.30V to varying positive potential limits, the hydrocortisone redox process was completely suppressed (Figure 4.36). This inhibitory behavior can be attributed to the sodium cations (Na⁺) which unlike the proton (H⁺) does not efficiently facilitate electron transfer in hydrocortisone redox system.

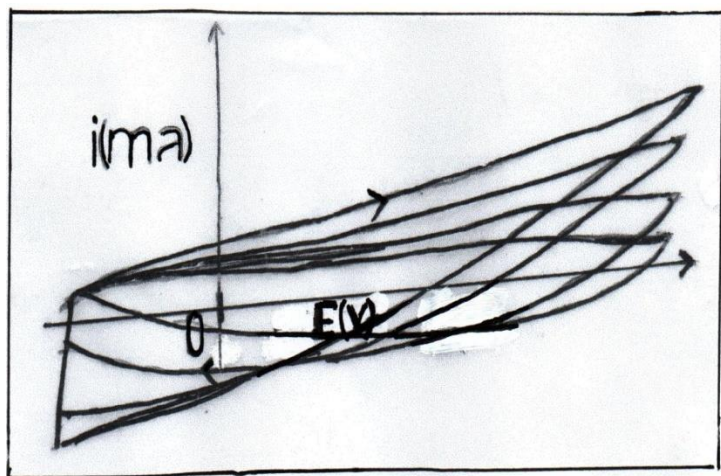


Figure 4.36: Cyclic voltammetric response of Hydrocortisone-PANI modified electrode in 0.1 M, 0.5M and 1.0M NaCl. Potential range: -0.30V to 0.90V. Scan rate 20mV/s. **CV Scale:** 0.09V/cm (x-axis): 0.02mA/cm (y-axis)

4.3.4. Electrochemical properties of Hydrocortisone on Bentonite modified electrode

The carbon graphite working electrode was modified using bentonite as already described in the Thesis. The bentonite modified electrode was further derivatised using hydrocortisone cream by dip coating. This electrode was transferred to a solution containing 1.0M H₂SO₄ and the potential cycled from -0.30V to 0.90V at varying scan rates. The resultant cyclic voltammetric response is shown in Figure 4.37. The redox profile is characterized by broad misshapened peaks. These poor faradaic processes are probably then result of restrictions in the ingress/egress of the hydrocortisone redox active moiety into the bentonite matrix. This restriction has an entropic effect which affects the Gibbs free energy of the redox process, hence affecting the redox potentials.

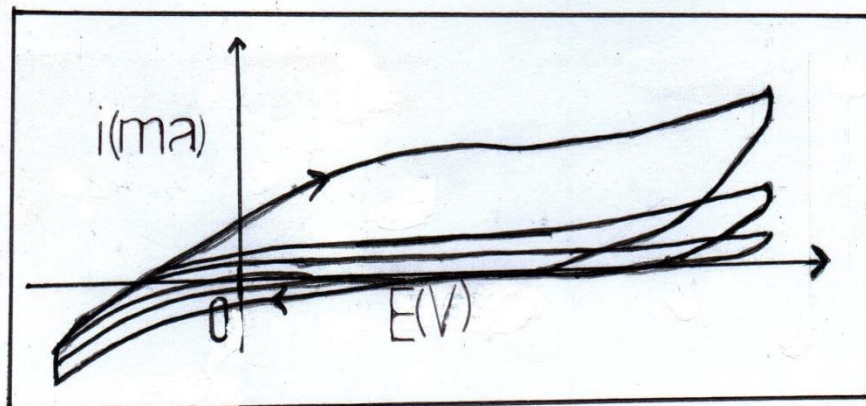


Figure 4.37: Cyclic voltammetric response of Hydrocortisone-Bentonite modified electrode in 1.0M H_2SO_4 . Potential range: -0.30V to 0.90V. Scan rate 20mV/s. **CV Scale:** 0.09V/cm (x-axis): 0.02mA/cm (y-axis)

The bentonite electrode was then modified using polyaniline by cycling its potential from -0.30V to 0.90V in a solution containing 0.1m aniline and 1.0M sulphuric acid at a scan rate of 20mV/s.

The resultant bentonite-polyaniline electrode was then modified with the hydrocortisone cream.

The potential of this electrode was then cycled from -0.30V to 0.90V in 1.0M sulphuric acid.

The cyclic voltammogram is characterized by two broad oxidation peaks at 0.40V and 0.74V which are relatively well defined at higher scan rates. There is a single broad misshapened peak at 0.31V (see Figure 4.38). It is apparent that the presence of polyaniline improves the redox behavior of hydrocortisone as compared to the case of bentonite modified electrode. This improvement in the redox behavior can be attributed to protonation –deprotonation equilibria imparted on the bentonite by the polyaniline.

4.3.5. Hydrocortisone-Bentonite composite as electrode modification material.

Hydrocortisone cream was mixed with bentonite in a 1:1 ratio(w/w) . the resultant slurry was then used to modify the carbon graphite working electrode. This electrode was then transferred to an electrolyte solution containing 0.1M NaCl. The potential was cycled from - 0.30V to varying positive potential limits (0.70V, 0.75V, 0.80V, 0.85V and 0.90V). The scan rate was kept constant at 20mV/s. The resultant cyclic voltammetric response is characterized by broad poorly defined peaks. See Figure 4.39.

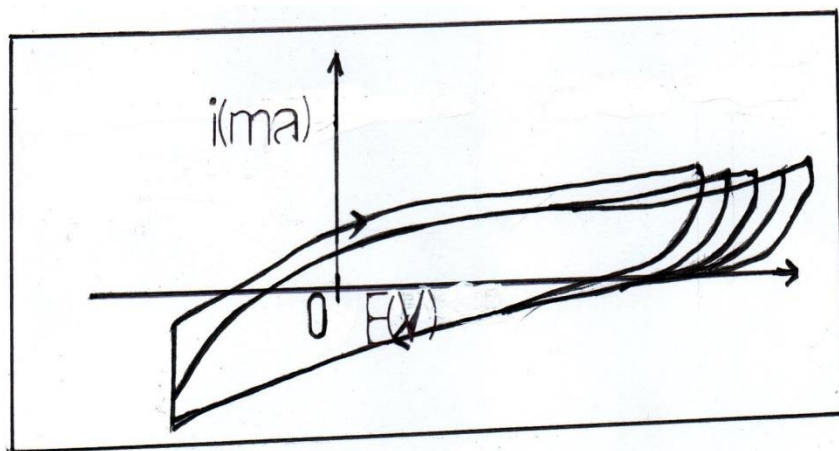


Figure 4.39: Cyclic voltammetric response of Hydrocortisone-Bentonite composite modified electrode in 0.1 M NaCl. Potential range: -0.30V to 0.90V. Scan rate 20mV/s. **CV Scale:** 0.09V/cm (x-axis): 0.02mA/cm (y-axis)

The redox properties of the hydrocortisone was not affect by variation of scan rate or tenfold increase in the concentration of the supporting electrolyte i.e., 1.0M NaCl. As already discussed Na^+ lack the versatility of H^+ , hence no improvement in the faradaic processes. To verify this assertion the electrode was now transferred to a supporting electrolyte solution containing 0.1M, 0.5M and 1.0M hydrochloric acid and the potential cycled from -0.30V to 0.90V at a scan rate of 50mV/s. Well-defined oxidation reduction peaks are now observed at 0.71V/0.63V. On continued variation of scan rate the oxidation and reduction peaks shifted positively by 20mV and negatively by 90mV respectively. This improvement in the redox process is attributed to the presence of protons. See Figure 4.40.

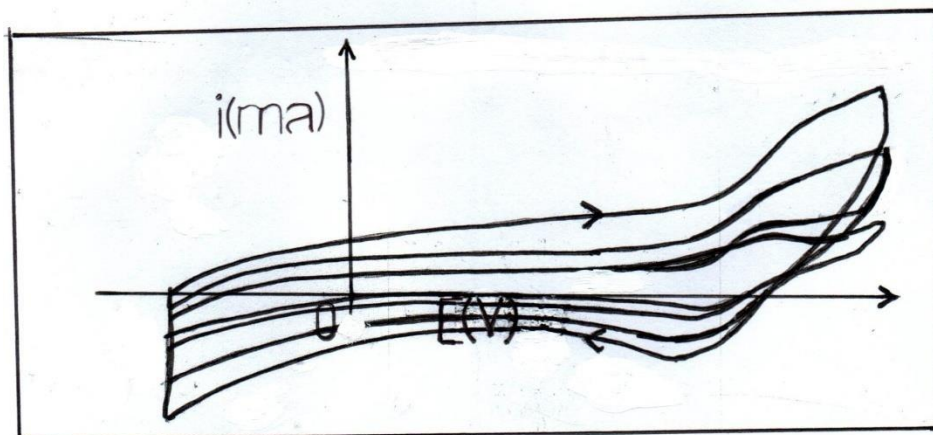


Figure 4.40: Cyclic voltammetric response of Hydrocortisone-Bentonite composite modified electrode in 1.0M NaCl. Potential range: -0.30V to 0.90V. Scan rate 20mV/s. **CV Scale:** 0.09V/cm (x-axis): 0.02mA/cm (y-axis)

When the variation of peak current is plotted versus the square root of scan rate, a linear plot is obtained suggesting that the redox process is diffusion limited.

On varying the positive potential limit in increments of 50mV, there was no change in the redox potentials, implying a stable entropic environment for the hydrocortisone in the bentonite matrix. This is expected given that bentonite is a clay montmorillonite characterized by well- structured tetrahedral and octahedral sites. Therefore inclusion of the hydrocortisone in the bentonite matrix as a result of composite formation ‘imposes/imparts’ lattice order on the bulky hydrocortisone molecule.

4.3.6. Redox activity of Hydrocortisone modified carbon graphite electrode in the presence of p-aminophenol

The carbon graphite working electrode was modified using hydrocortisone as already discussed. The hydrocortisone modified electrode had its potential cycled from -0.30 V to 0.90V at a scan rate of 20mv/s, in a solution containing 1.0M H₂S0₄ and 0.01M p-aminophenol. The resultant cyclic voltammetric response is shown in Figure 4.41.

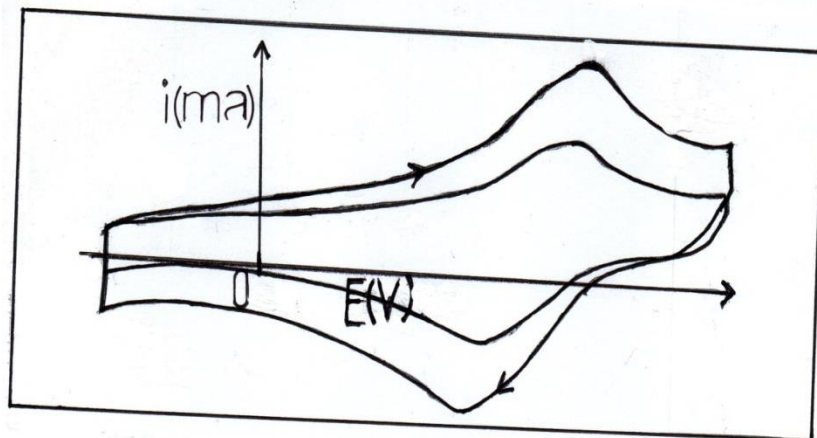


Figure 4.41: Cyclic voltammetric response of Hydrocortisone modified electrode in a solution containing 1.0M H_2SO_4 and 0.01M p-aminophenol. Potential range: -0.30V to 0.90V. Scan rate 20mV/s. **CV Scale:** 0.09V/cm (x-axis): 0.02mA/cm (y-axis)

An oxidation peak is observed at 0.67V and a corresponding reduction peak at 0.45V. It is proposed that the oxidation and reduction peaks correspond to the hydrocortisone redox process. Since in the absence of p-aminophenol this oxidation peak is not observed, the presence of p-aminophenol electro-catalyzes the hydrocortisone redox process by removing the oxidative stress. The reduction peak at 0.45V is attributable to the hydrocortisone reduction process. This peak is assumed to correspond to the reduction peak observed at 0.50V in the absence of p-aminophenol. It is proposed that p-aminophenol redox centers interact with the hydrocortisone redox centers leading to a lowering in the Gibbs free energy of the redox system, hence reduction in the reduction potential. This electro catalytic activity of the p-aminophenol bridges the energy gap between the redox centers, hence explaining the merger of the two reduction peaks observed earlier into one.

4.4 FTIR SPECTROPHOTOMETRIC ANALYSIS

4.4.1

FTIR analysis was conducted on Top lemon, Extra Clair and Hydrocortisone. The resultant FTIR spectral profiles are shown in Figures 4.48, 4.49 and 4.50.

In all the samples well defined **hydroxyl** spectral bands were observed in the range from 3260 cm^{-1} to 3298 cm^{-1} , for **aromatic bands** the range was 1625 cm^{-1} -1635 cm^{-1} and 1510- 1512 cm^{-1} .

Absorption peaks representing **saturated hydrocarbon** was observed in the range 2851-2916 cm^{-1} Spectral band in the range of 1045 cm^{-1} -1222 cm^{-1} representing **C-O stretch** was also observed in all the cases. The presence of a these spectral bands is in agreement with electrochemical data.

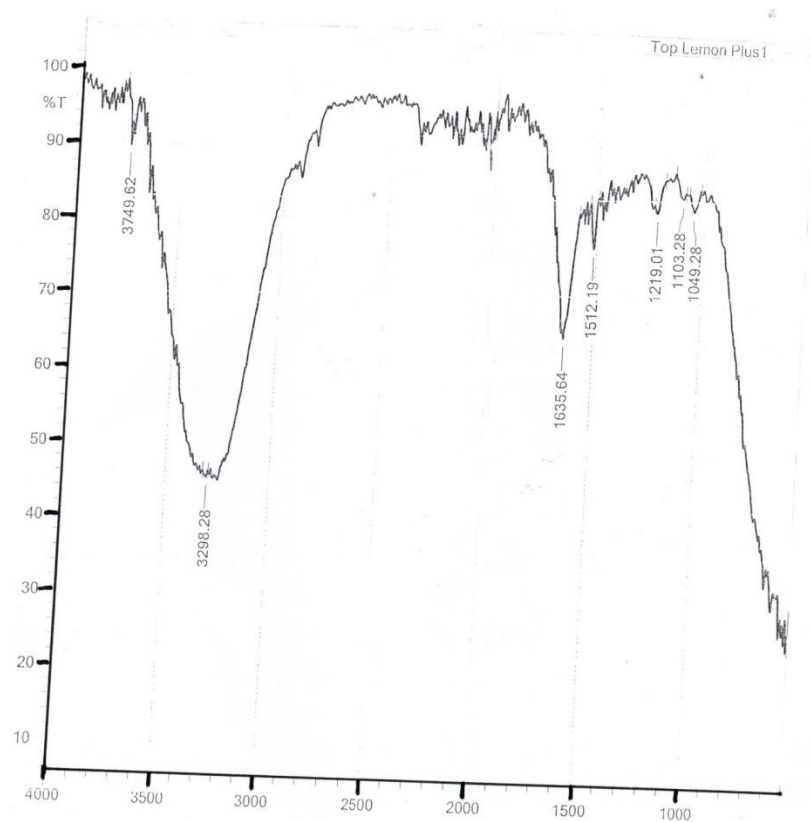


Figure 4.42: FTIR spectral data for Top lemon

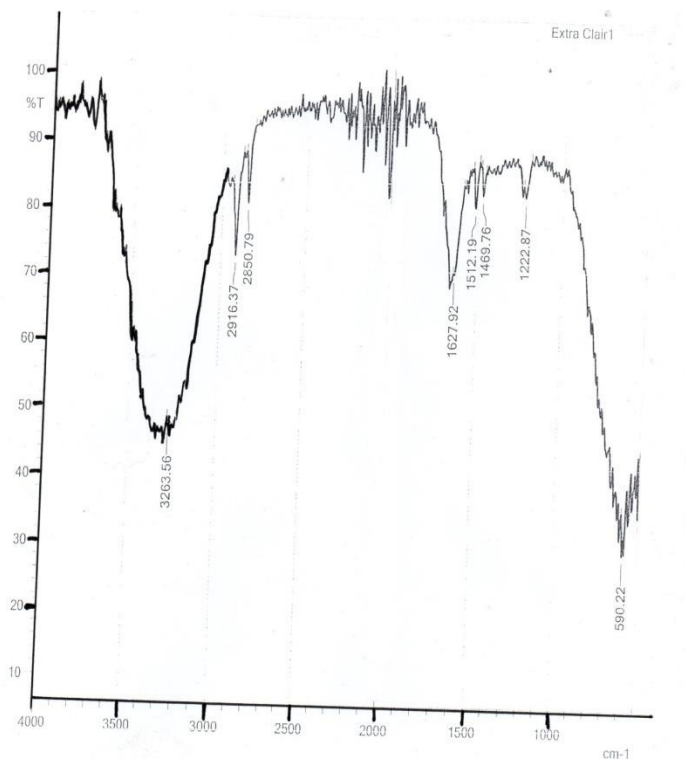


Figure 4.43: FTIR spectral data for Extra Clair

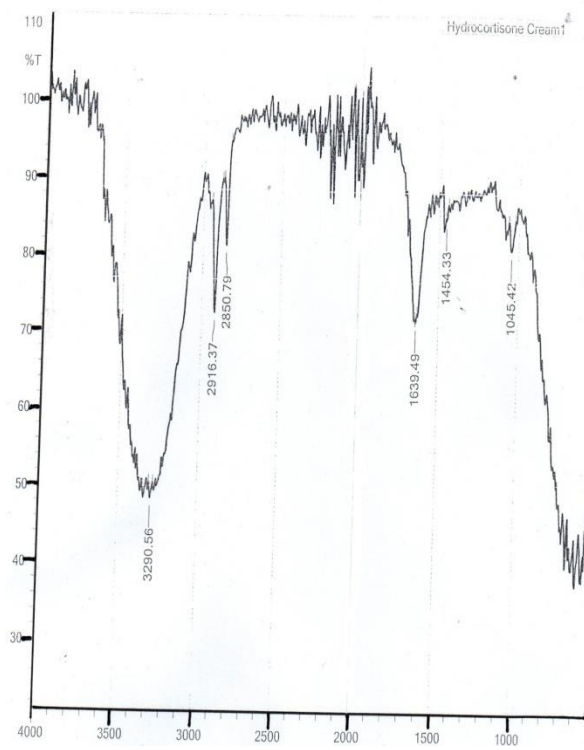


Figure 4.43: FTIR spectral data for Hydrocortisone cream

CHAPTER FIVE

CONCLUSION AND RECOMMENDATIONS

5.1 CONCLUSION

The results presented in this thesis, confirm the versatility of surface modified electrodes as a Nano-electroanalytical tool in profiling the electrochemical activity of redox active moieties in Hydrocortisone (Medicated cream), Top-lemon and Extra Clair (Beauty creams).

The detection of Quinone derivatives in beauty creams using conventional chemical methods has always posed significant challenges, hence the detection of these derivatives using surface modified electrodes opens a new analytical frontier.

This significance is further captured in the fact that very low quantities of hydroquinone are detected i.e., 3.57×10^{-5} g. This confirms the 'Nano'- detection element of surface modified electrodes.

The use of host matrices such as electronically conducting polymers (polyaniline) and bentonite (clay montmorillonite) and the resultant enhancement in the electrochemical signal associated with the redox moieties in the creams due to pre-concentration and a combination of structural and entropic effects introduces lays the foundation for surface modified electrodes as Nano-electroanalytical tools.

5.2 RECOMMENDATIONS

It is suggestive therefore, that the applications domain of surface modified electrodes as a nano-electroanalytical tool be refined and expanded to include the analysis of a broad spectrum of chemical products containing redox active moieties. In addition new host matrices are considered with the focus being on their ability to improve the redox signal levels for the redox active moieties in the analyte.

REFERENCES

- Adams R.W., (1969), Electrochemistry at solid electrodes monographs in electroanalytical chemistry and electrochemistry ed. by Bard A. J., Marcel Dekker NY.
- Adriana M., Erika S., Domenica T., (2006), Electrodeposited glucose oxidase/anionic clay for glucose biosensors design, *AnalyticaChimicaActa*: **577**, 98-106.
- Arnold B.B. and Murphy G.W., (1965), Studies on the electrochemistry of carbon and chemically modified carbon surfaces, *J. Phys. Chem.*:**65**, 135-136.
- Bakhshi A.K. and Rattan P., (1997), Electrical conducting polymers: an emerging technology, *Curr.Sc.***73**, 648.
- Bard A.J. and Rudzinski W.E., (1986), Clay modified electrodes, Part VI: aluminium and silicon pillared clay modified electrodes, *J.Electroanal. Chem*: **199**, 323-340
- Bontidean I., Ahlqvist J. Mulchandani A., Chen W., Bae W., Mehra R.K., Mortari A., Csoregi E., (2003), Novel synthetic phytochelatin-based capacitive biosensor for heavy metal ion detection, *Biosens. Bioelectron*:**18**, 547-553.
- Bontidean I., Berggren C., Johansson G., Csoregi E., Mattiasson B., Lloyd J.R., Jakeman K.J., Brown N. L., (1998), Detection of heavy metal ions at femtomolar levels using protein-based biosensors. *Anal. Chem*: **70**: 4162-4164.
- Carter M.T. and Bard A.J., (1986), Clay Modified Electrodes. Part VII. The Electrochemical Behavior of Tetrathiafulvalenium-montrillonite Modified Electrodes, *J. Electroanal. Chem*:**229**, 191-214.
- Chow E. J. and Gooding J. (2006), Peptide modified electrodes as electrochemical metal ion sensors, *Electroanalysis*:**18**, 1437 – 1448.
- Daisuke O. and Susumu K. (2007), Preparation of Selective Micro glucose sensor without permselective membrane by electrochemical deposition of Ruthenium and glucose oxidase *Electrochemistry Communications*: **9**, 1012-1016.

- Ege D., Gosh P.K., White J.R., Equey J.F. and Bard A.J., (1984), Clay Modified Electrodes 3: Electrochemical and Electron Spin Resonance Studies of Montmorillonite Layers, *J. Am. Chem. Soc.*: **107**, 5644-5646.
- Elliot C.M. and Murray R. W, (1976), Chemically Modified Carbon Electrodes, *Anal. Chem.*: **48**, 1247.
- Evans J.F., Kuwana T., Henne M.T., and Royer J.P., 1977, Electrocatalysis of solution species using modified electrodes, *J. Electroanal. Chem. Soc.*: 80, 409-416
- Firth B. E., Murray R.W., Miller L.L., Mitani M., Rogers T. and Lennox J., (1976), Anodic and cathodic reactions on a chemically modified edge surface of graphite, *J. Am. Chem. Soc.*: **98**, 8271-8274.
- Gosh P.K. and Bard A.J., (1983), Clay Modified Electrodes part II, *J. Electroanal. Chem. Soc.*: **105**, 5691-5693.
- Heinz J. and Merz A. (1990), Topics in Current Chemistry, Springer Verlag Berlin.
- Lane R.F. and Hubbard A.T., (1973), Electrochemistry of Chemisorbed Molecules. Reactants Connected to Electrodes through Olefinic Substituents and Influence of Charged Chemisorbed Molecules on the Electrode Reactions of Platinum Complexes, *J. Phys. Chem.*: **77**, 1401-1421.
- Lennox J.C. and Murray R.W., (1977), Chemically Modified Electrode. Electron spectroscopy for chemical analyses and alternating current voltammetry of glassy carbon- bound tetra (amino phenyl) porphyrins. *J. Am. Chem. Soc.*: **100**, 3710.
- Orata, D.O., (1989), Effects of pyridine on porosity and redox properties of poly-thiophene. *Bull. Chem. Soc. Ethiop.*: **3** (1).
- Orata D., Yusuf a., Nineza C., (2014) Derivatised Electrodes in Electroanalysis of Pyrimethamine/2-sulfailido-3-methoxypyrazine and Lumefantrine/Artemeter, *J. Chem. Chem Eng.*: Vol.8, Pg 215-225.**
- Orata D., Yusuf A., Nineza C., Mukabi M., Njenga H., Mbui D., (2014) Surface modified electrode used in the electro-analysis of N- Acetyl P-Aminophenol- A pharmaceutical drug. *IOSR J. Appl. Chem.*: Vol. 7 Pg 90-99.**

Orata D., Yusuf A., Mukabi M., H. Njenga H., Mbui D., Electro-characterization of polypyrrole electro synthesized on a montmorillonite host-matrix, in aqueous media containing sulphuric acid as supporting electrolyte. *IOSR J. Appl. Chem: Vol.7 Pg. 59-72.*

Orata D., Yusuf A., Nineza C., Mukabi M., Njenga H., Mbui D., (2014) Surface modified electrodes used in cyclic voltammetric profiling of quinine an anti-malarial drug. *IOSR J. Appl. Chem: Vol. 7 (2014) Pg 54-58.*

Orata D. O. and Okongo E., (2000), Allen- Hickling equation applied to the quasi-reversible polyaniline redox, *Reactive and Functional Polymers:45*, Issue 3, 211-216.

Orata D. O., (1992), Electrochemical characteristics of polyaniline electro polymerized on a phenol modified carbon electrode. *Bull. Chem. Soc. Ethiop:6* ,1.

Orata D.O. and Buttery D.A., (1987), Determination of ion population and solvent content as a function of redox state and pH in polyaniline, *J.Am.Chem. Soc: 109*, 357.

Orata, D.O and Segor F. (1999), Bentonite as a template for electro- synthesis of thyroxine *Catalysis letter:58*, 157- 163.

Oyama N. and Anson F. C., (1980), Facile attachment of transition metal complexes to graphite electrodes coated with polymer ligands. Observation and control of metal-ligand-coordination among reactants confined to electrode surface. *J. Am. Chem. Soc:101*, 739

P.W. Atkins (1998) 'Physical Chemistry', 6th Edition, Oxford University Press.

Riul A. Jr., Gallardo A. M. S., Mello S. V., Bone S., Taylor D. M. and Mattoso L. H. C, (2003), An electronic tongue using polypyrrole and polyaniline, *Synthetic Metals:132*, 109-116.

Willard H. H., Meritt L. L. Dean J. A. and Settle F. A., (1986), 'Instrumental Methods of Analysis', 6th Edition, pp. 632-639. CBS, Delhi, India.

Wikipedia, Google Internet

APPENDIX

CALCULATION OF THE ELECTROGRAVIMETRIC WEIGHT OF HYDROQUINONE IN TOP LEMON CREAM

Q_{ox} value computed from the cyclic voltammogram of Top lemon was $4 \times 10^{-6} \text{ C/cm}^2$

Since $\tau = \frac{Q_{ox}}{nFA}$, where n is the number of electrons, F is the Faradays constant and A the surface area of the carbon graphite working electrode (0.38 cm^2)

Assuming $n = 1$ for the quinone redox process i.e., $2H + /e$

$$\tau = 1.1 \times 10^{-11} \text{ mol/cm}^2$$

Assuming the molecular weight of hydroquinone is 110 g/mol

$$\tau \times \text{Mwt HyQ} = 1.21 \times 10^{-8} \text{ mol/cm}^2$$

Uniform spread analysis for Top lemon gave the value of $0.13 \text{ g Top lemon} = 25.5 \text{ cm}^3$

$$\tau = 3.1 \times 10^{-7} \text{ g}$$

$$\% \text{ Hydroquinone} = 3.1 \times 10^{-7} \text{ g} / 0.13 \text{ g} \times 100 = 0.0001\%$$

The total mass of Top lemon in the tube = 15 g

$$\text{Total amount of hydroquinone in the tube} = 3.1 \times 10^{-7} \text{ g} / 0.13 \text{ g} \times 15 = 3.57 \times 10^{-5} \text{ g}$$